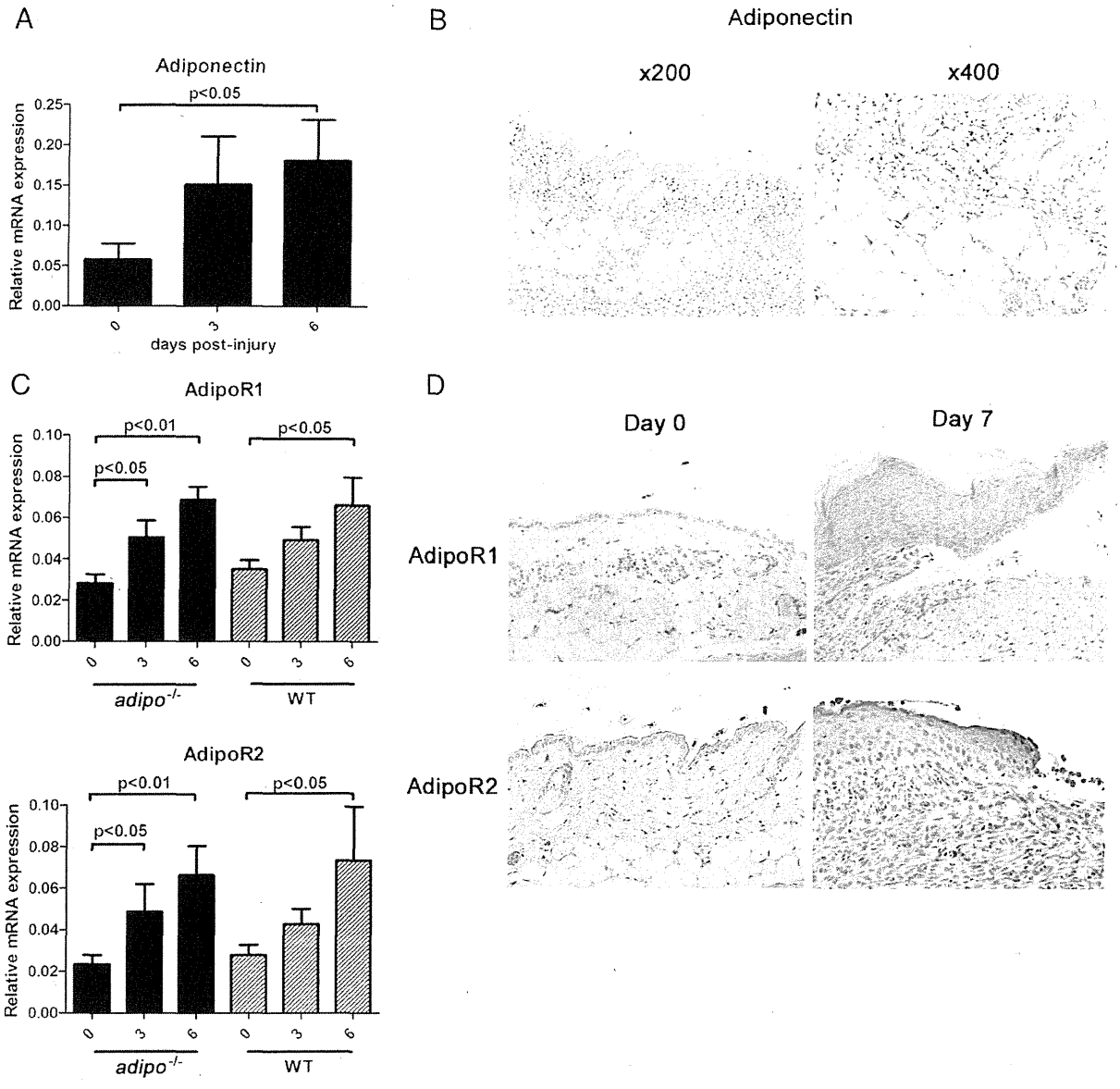

FIGURE 7. Regulation of adiponectin and AdipoR1/AdipoR2 mRNA expression during wound repair. Skin samples were taken immediately before (at day 0) and 3 and 6 d (days 3 and 6) after wounding from wild-type and adiponectin-deficient mice. Gene expression levels of adiponectin (**A**) and AdipoR1/ AdipoR2 (**C**) were analyzed by the qrt-PCR. Immunohistochemistry for adiponectin (**B**) at day 7 in wild-type mice and AdipoR1/ AdipoR2 (**D**) at days 0 and 7 in wild-type and adiponectin-deficient mice was performed (original magnification ×400).

Discussion

Adiponectin, a key mediator in the pathogenesis of diabetes, exerts multiple biological activities in various diseases; however, its role in cutaneous wound healing is unknown. To clarify this, we investigated pathophysiologic roles of adiponectin during cutaneous wound healing. We first demonstrated that keratinocytes express adiponectin receptors and that adiponectin induces proliferation and migration of keratinocytes in a dose-dependent manner through ERK activation in vitro. By using siRNAs of adiponectin receptors on keratinocytes, we also determined that AdipoR1 and AdipoR2 are mainly involved in the adiponectin-mediated ERK signaling pathway. These in vitro results suggest that adiponetin might contribute to the re-epithelialization phase of optimal wound healing. We have next undertaken a detailed functional analysis of adiponectin during wound repair in vivo. Wound closure was significantly delayed in adiponectin-deficient mice compared with wild-type mice. The number of Ki67-positive cells in the wound margin epithelial cells was decreased and re-epithelialization was delayed in adiponectin-deficient mice, which were supportive of in vitro results. The expression of AdipoR1/AdipoR2 as well as adiponectin gradually increased after wounding, which may consequently augment adiponectin signaling within keratinocytes and facilitate wound repair. Finally, we examined the curative effect of adiponectin on wounds. Both systemic and topical adiponectin supplementation normalized the impaired wound healing in adiponectin-deficient mice and *db/db* mice, respectively. Thus, adiponectin might contribute to optimal cutaneous wound healing in diabetic patients, whose adiponectin levels are persistently decreased.

With regard to cell proliferation and migration, the behavior of adiponectin seems to depend on cell types. For instance, adiponectin stimulates cell growth in colonic epithelial cells (39), osteoblasts (40), and cardiac fibroblasts (41), where adiponectin is involved in the gastrointenstinal mucosal metabolism, bone me-

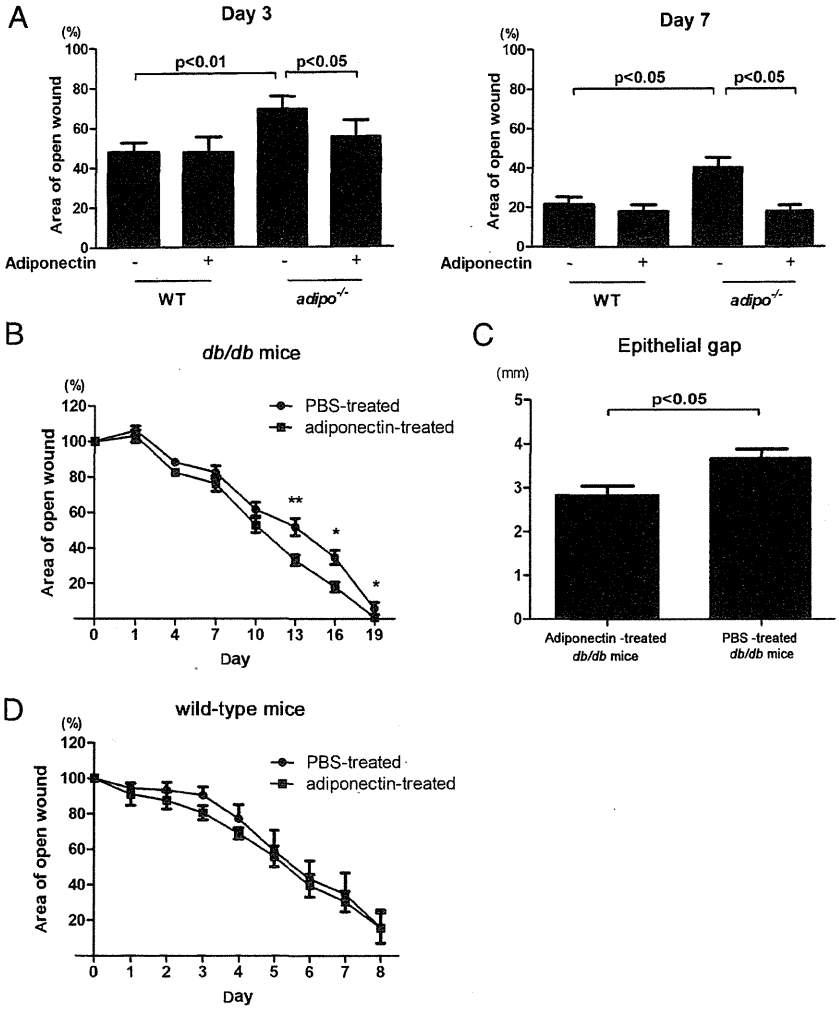

FIGURE 8. Effect of systemically and topically supplemented adiponectin on wound healing in wild-type, adiponectin-deficient, and *db/db* mice. (**A**) Wild-type and adiponectin-deficient mice were given daily i.p. injection of recombinant adiponectin (50 μg/day), and the area of open wound was measured at days 3 and 7 after wounding. Thirteen wounds from six wild-type and 14 wounds from six adiponectin-deficient mice were used for the analysis. Data are shown as mean ± SE. (**B**) *db/db* mice were given daily topical administration of PBS with or without recombinant adiponectin (2.5 μg/day), and the area of open wound was measured after wounding. Data are shown as mean ± SE, obtained from five *db/db* mice (10 wounds for adiponectin-treated and PBS-treated group, respectively). (**C**) The epithelial gap was microscopically measured in the skin sections taken 13 d after wounding of *db/db* mice. Data are shown as mean ± SE, obtained from five *db/db* mice (10 wounds for adiponectin-treated and PBS-treated group, respectively). (**D**) Wild-type mice were given daily topical administration of PBS with or without recombinant adiponectin (2.5 μg/day), and the area of open wound was measured after wounding. Data are shown as mean ± SE, obtained from five wild-type mice (10 wounds for adiponectin-treated and PBS-treated group, respectively).

tabolism, and myocardial hypertrophy, respectively. Migratory effects of adiponectin have been reported in endothelial progenitor cells (44). In contrast, adiponectin suppressed cell proliferation and migration in vascular smooth muscle cells (45) and hepatic stellate cells (46), acting as a modulator for vascular remodeling and liver fibrosis, respectively. Most importantly, a certain subset of cell types that are involved in the cutaneous wound healing process exhibit proliferative and migratory behaviors in response to adiponectin. Dermal fibroblasts are the dominant players in the process of granulation tissue formation during cutaneous wound healing. Recent reports have revealed that adiponectin induces proliferation of dermal fibroblasts and upregulation of collagen production (47, 48). Furthermore, adiponectin induces proliferation of HUVECs and stimulates angiogenesis (10), indicating the positive contribution of adiponectin to optimal wound repair. In addition, adiponectin induces neutrophil migration, which is an initial step of skin wound repair (14). In this study, adiponectin exhibited proliferative and migratory effects on primary human keratinocytes. Proliferation and migration of keratinocytes are crucial factors of re-epithelialization, which marks the final stage of wound healing (14). Given that inflammation, granulation tissue formation, re-epithelialization, and angiogenesis are sequential central events, adiponectin may play a vital role throughout the wound healing process. It should be mentioned that Kawai et al. (49) previously reported that adiponectin slightly suppressed the proliferation of the immortalized keratinocyte cell line HaCaT. Therefore, we also investigated whether adiponectin would exert effects on HaCaT cells as well; however, in our hands, adiponectin had no effect on proliferation of these cells (Supplemental Fig. 1). Although the reason for the discrepancy of the results between primary normal human keratinocytes and HaCaT cells is not clear, HaCaT cells have been reported to behave differently from normal human keratinocytes regarding cell growth, differentiation, and cytokine production in several reports (50, 51).

Consistent with our in vitro results, a significant impairment of wound repair was also observed in adiponectin-deficient mice in the current study. Furthermore, both systemic and topical adiponcetin accelerated wound repair in adiponectin-deficient and diabetic *db/db* mice, respectively. In contrast, the wound closure rate of wild-type mice did not change after systemic or local administration of adiponectin. Thus, adiponectin has beneficial and direct effects on cutaneous wound healing, especially in diabetic patients whose adiponectin levels are constitutively decreased. These findings would suggest that upregulating serum adiponectin levels through medical treatment as well as raising cutaneous local adiponectin levels by direct administration of adiponectin to the wound sites represents a novel effective therapeutic target for delayed diabetic wounds (52).

There has been no information available regarding the adiponectin-induced intracellular signaling in keratinocytes. The signaling pathways involved in cell proliferation and migration by adiponectin are tissue-/cell type-specific, including p38 MAPK,

JNK, ERK, PI3K, and Akt (10, 39–41). In the current study, we demonstrate that the proliferative and migratory activities of adiponectin are mediated through ERK signaling. It has been reported that the ERK signaling pathway is activated as a downstream signal molecule of adiponectin receptors in several cell types, including endothelial cells, macrophages, cardiac fibroblasts, and pancreatic cells (10, 41, 53, 54). Previous studies have shown that the ERK signaling pathway is activated upon injury or stretching of keratinocytes (55, 56). Interestingly, ERK pathways are required for wound healing in corneal epithelial cells under high glucose conditions (57). Considering that ERK activation is required for keratinocyte proliferation and migration (58), our present result showing that adiponectin activates the ERK signaling pathway in keratinocytes would suggest that adiponectin positively regulates the re-epithelialization process during cutaneous wound healing.

In summary, we propose a potent role for adiponectin, a key mediator of diabetes, in the regulation of keratinocyte proliferation and migration during cutaneous wound healing and provide a new mechanism underlying delayed wound repair in diabetic patients. On the basis of our data, we propose that systemic and/or local upregulation of adiponectin levels may represent a novel therapeutic strategy for diabetic wounds.

Acknowledgments

We thank Dr. Wolfgang W. Leitner (National Institute of Allergy and Infectious Diseases, National Institutes of Health) for helpful discussions.

Disclosures

The authors have no financial conflicts of interest.

References

1. Klein, J., P. A. Permana, M. Owecki, G. N. Chaldakov, M. Böhm, G. Hausman, C. M. Lapière, P. Atanassova, J. Sowiński, M. Fasshauer, et al. 2007. What are subcutaneous adipocytes really good for? *Exp. Dermatol.* 16: 45–70.
2. Scherer, P. E. 2006. Adipose tissue: from lipid storage compartment to endocrine organ. *Diabetes* 55: 1537–1545.
3. Kadowaki, T., T. Yamauchi, and N. Kubota. 2008. The physiological and pathophysiological role of adiponectin and adiponectin receptors in the peripheral tissues and CNS. *FEBS Lett.* 582: 74–80.
4. Yamauchi, T., J. Kamon, Y. Minokoshi, Y. Ito, H. Waki, S. Uchida, S. Yamashita, M. Noda, S. Kita, K. Ueki, et al. 2002. Adiponectin stimulates glucose utilization and fatty-acid oxidation by activating AMP-activated protein kinase. *Nat. Med.* 8: 1288–1295.
5. Kadowaki, T., T. Yamauchi, N. Kubota, K. Hara, K. Ueki, and K. Tobe. 2006. Adiponectin and adiponectin receptors in insulin resistance, diabetes, and the metabolic syndrome. *J. Clin. Invest.* 116: 1784–1792.
6. Kubota, N., Y. Terauchi, T. Yamauchi, T. Kubota, M. Moroi, J. Matsui, K. Eto, T. Yamashita, J. Kamon, H. Satoh, et al. 2002. Disruption of adiponectin causes insulin resistance and neointimal formation. *J. Biol. Chem.* 277: 25863–25866.
7. Hotta, K., T. Funahashi, Y. Arita, M. Takahashi, M. Matsuda, Y. Okamoto, H. Iwahashi, H. Kuriyama, N. Ouchi, K. Maeda, et al. 2000. Plasma concentrations of a novel, adipose-specific protein, adiponectin, in type 2 diabetic patients. *Arterioscler. Thromb. Vasc. Biol.* 20: 1595–1599.
8. Shibata, R., K. Sato, M. Kumada, Y. Izumiya, M. Sonoda, S. Kihara, N. Ouchi, and K. Walsh. 2007. Adiponectin accumulates in myocardial tissue that has been damaged by ischemia-reperfusion injury via leakage from the vascular compartment. *Cardiovasc. Res.* 74: 471–479.
9. Ohashi, K., H. Iwatani, S. Kihara, Y. Nakagawa, N. Komura, K. Fujita, N. Maeda, M. Nishida, F. Katsube, I. Shimomura, et al. 2007. Exacerbation of albuminuria and renal fibrosis in subtotal renal ablation model of adiponectin-knockout mice. *Arterioscler. Thromb. Vasc. Biol.* 27: 1910–1917.
10. Ouchi, N., H. Kobayashi, S. Kihara, M. Kumada, K. Sato, T. Inoue, T. Funahashi, and K. Walsh. 2004. Adiponectin stimulates angiogenesis by promoting cross-talk between AMP-activated protein kinase and Akt signaling in endothelial cells. *J. Biol. Chem.* 279: 1304–1309.
11. Jeffcoate, W. J., and K. G. Harding. 2003. Diabetic foot ulcers. *Lancet* 361: 1545–1551.
12. Kämpfer, H., R. Schmidt, G. Geisslinger, J. Pfeilschifter, and S. Frank. 2005. Wound inflammation in diabetic ob/ob mice: functional coupling of prostaglandin biosynthesis to cyclooxygenase-1 activity in diabetes-impaired wound healing. *Diabetes* 54: 1543–1551.
13. Falanga, V. 2005. Wound healing and its impairment in the diabetic foot. *Lancet* 366: 1736–1743.
14. Singer, A. J., and R. A. Clark. 1999. Cutaneous wound healing. *N. Engl. J. Med.* 341: 738–746.
15. Yamashita, H., S. Oh-ishi, T. Kizaki, J. Nagasawa, D. Saitoh, Y. Ohira, and H. Ohno. 1995. Insulin stimulates the expression of basic fibroblast growth factor in rat brown adipocyte primary culture. *Eur. J. Cell Biol.* 68: 8–13.
16. Zizola, C. F., M. E. Balañá, M. Sandoval, and J. C. Calvo. 2002. Changes in IGF-I receptor and IGF-I mRNA during differentiation of 3T3-L1 preadipocytes. *Biochimie* 84: 975–980.
17. Matsuzawa, Y. 2006. The metabolic syndrome and adipocytokines. *FEBS Lett.* 580: 2917–2921.
18. Kosacka, J., M. Nowicki, J. Kacza, J. Borlak, J. Engele, and K. Spanel-Borowski. 2006. Adipocyte-derived angiopoietin-1 supports neurite outgrowth and synaptogenesis of sensory neurons. *J. Neurosci. Res.* 83: 1160–1169.
19. Fu, X., L. Fang, H. Li, X. Li, B. Cheng, and Z. Sheng. 2007. Adipose tissue extract enhances skin wound healing. *Wound Repair Regen.* 15: 540–548.
20. Frank, S., B. Stallmeyer, H. Kämpfer, N. Kolb, and J. Pfeilschifter. 2000. Leptin enhances wound re-epithelialization and constitutes a direct function of leptin in skin repair. *J. Clin. Invest.* 106: 501–509.
21. Stallmeyer, B., H. Kämpfer, M. Podda, R. Kaufmann, J. Pfeilschifter, and S. Frank. 2001. A novel keratinocyte mitogen: regulation of leptin and its functional receptor in skin repair. *J. Invest. Dermatol.* 117: 98–105.
22. Yamauchi, T., J. Kamon, H. Waki, Y. Terauchi, N. Kubota, K. Hara, Y. Mori, T. Ide, K. Murakami, N. Tsuboyama-Kasaoka, et al. 2001. The fat-derived hormone adiponectin reverses insulin resistance associated with both lipoatrophy and obesity. *Nat. Med.* 7: 941–946.
23. Shirakata, Y., T. Komurasaki, H. Toyoda, Y. Hanakawa, K. Yamasaki, S. Tokumaru, K. Sayama, and K. Hashimoto. 2000. Epiregulin, a novel member of the epidermal growth factor family, is an autocrine growth factor in normal human keratinocytes. *J. Biol. Chem.* 275: 5748–5753.
24. Shibata, S., Y. Tada, N. Kanda, K. Nashiro, M. Kamata, M. Karakawa, T. Miyagaki, H. Kai, H. Saeki, Y. Shirakata, et al. 2010. Possible roles of IL-27 in the pathogenesis of psoriasis. *J. Invest. Dermatol.* 130: 1034–1039.
25. Takahata, C., Y. Miyoshi, N. Irahara, T. Taguchi, Y. Tamaki, and S. Noguchi. 2007. Demonstration of adiponectin receptors 1 and 2 mRNA expression in human breast cancer cells. *Cancer Lett.* 250: 229–236.
26. Taguchi, J., A. Fujii, Y. Fujino, Y. Tsujioka, M. Takahashi, Y. Tsuboi, I. Wada, and T. Yamada. 2000. Different expression of calreticulin and immunoglobulin binding protein in Alzheimer's disease brain. *Acta Neuropathol.* 100: 153–160.
27. Takeuchi, T., S. B. Liang, N. Matsuyoshi, S. Zhou, Y. Miyachi, H. Sonobe, and Y. Ohtsuki. 2002. Loss of T-cadherin (CDH13, H-cadherin) expression in cutaneous squamous cell carcinoma. *Lab. Invest.* 82: 1023–1029.
28. Fujimoto, S., H. Uratsuji, H. Saeki, S. Kagami, Y. Tsunemi, M. Komine, and K. Tamaki. 2008. CCR4 and CCR10 are expressed on epidermal keratinocytes and are involved in cutaneous immune reaction. *Cytokine* 44: 172–178.
29. Boyden, S. 1962. The chemotactic effect of mixtures of antibody and antigen on polymorphonuclear leucocytes. *J. Exp. Med.* 115: 453–466.
30. Yamauchi, T., J. Kamon, Y. Ito, A. Tsuchida, T. Yokomizo, S. Kita, T. Sugiyama, M. Miyagishi, K. Hara, M. Tsunoda, et al. 2003. Cloning of adiponectin receptors that mediate antidiabetic metabolic effects. *Nature* 423: 762–769.
31. Denzel, M. S., M. C. Scimia, P. M. Zumstein, K. Walsh, P. Ruiz-Lozano, and B. Ranscht. 2010. T-cadherin is critical for adiponectin-mediated cardioprotection in mice. *J. Clin. Invest.* 120: 4342–4352.
32. Lee, M. H., R. L. Klein, H. M. El-Shewy, D. K. Luttrell, and L. M. Luttrell. 2008. The adiponectin receptors AdipoR1 and AdipoR2 activate ERK1/2 through a Src/Ras-dependent pathway and stimulate cell growth. *Biochemistry* 47: 11682–11692.
33. Maruyama, S., R. Shibata, K. Ohashi, T. Ohashi, H. Daida, K. Walsh, T. Murohara, and N. Ouchi. 2011. Adiponectin ameliorates doxorubicin-induced cardiotoxicity through Akt protein-dependent mechanism. *J. Biol. Chem.* 286: 32790–32800.
34. Ohashi, K., N. Ouchi, K. Sato, A. Higuchi, T. O. Ishikawa, H. R. Herschman, S. Kihara, and K. Walsh. 2009. Adiponectin promotes revascularization of ischemic muscle through a cyclooxygenase 2-dependent mechanism. *Mol. Cell. Biol.* 29: 3487–3499.
35. Ouchi, N., and K. Walsh. 2008. A novel role for adiponectin in the regulation of inflammation. *Arterioscler. Thromb. Vasc. Biol.* 28: 1219–1221.
36. Kelesidis, I., T. Kelesidis, and C. S. Mantzoros. 2006. Adiponectin and cancer: a systematic review. *Br. J. Cancer* 94: 1221–1225.
37. Wenczak, B. A., J. B. Lynch, and L. B. Nanney. 1992. Epidermal growth factor receptor distribution in burn wounds: implications for growth factor-mediated repair. *J. Clin. Invest.* 90: 2392–2401.
38. Matsumoto, K., K. Hashimoto, K. Yoshikawa, and T. Nakamura. 1991. Marked stimulation of growth and motility of human keratinocytes by hepatocyte growth factor. *Exp. Cell Res.* 196: 114–120.
39. Ogunwobi, O. O., and I. L. Beales. 2006. Adiponectin stimulates proliferation and cytokine secretion in colonic epithelial cells. *Regul. Pept.* 134: 105–113.
40. Luo, X. H., L. J. Guo, L. Q. Yuan, H. Xie, H. D. Zhou, X. P. Wu, and E. Y. Liao. 2005. Adiponectin stimulates human osteoblasts proliferation and differentiation via the MAPK signaling pathway. *Exp. Cell Res.* 309: 99–109.
41. Hattori, Y., S. Hattori, K. Akimoto, T. Nishikimi, K. Suzuki, H. Matsuoka, and K. Kasai. 2007. Globular adiponectin activates nuclear factor-κB and activating protein-1 and enhances angiotensin II-induced proliferation in cardiac fibroblasts. *Diabetes* 56: 804–808.
42. Gerdes, J., H. Lemke, H. Baisch, H. H. Wacker, U. Schwab, and H. Stein. 1984. Cell cycle analysis of a cell proliferation-associated human nuclear antigen defined by the monoclonal antibody Ki-67. *J. Immunol.* 133: 1710–1715.

43. Tsuboi, R., and D. B. Rifkin. 1990. Recombinant basic fibroblast growth factor stimulates wound healing in healing-impaired db/db mice. *J. Exp. Med.* 172: 245–251.
44. Nakamura, N., K. Naruse, T. Matsuki, Y. Hamada, E. Nakashima, H. Kamiya, T. Matsubara, A. Enomoto, M. Takahashi, Y. Oiso, and J. Nakamura. 2009. Adiponectin promotes migration activities of endothelial progenitor cells via Cdc42/Rac1. *FEBS Lett.* 583: 2457–2463.
45. Arita, Y., S. Kihara, N. Ouchi, K. Maeda, H. Kuriyama, Y. Okamoto, M. Kumada, K. Hotta, M. Nishida, M. Takahashi, et al. 2002. Adipocyte-derived plasma protein adiponectin acts as a platelet-derived growth factor-BB-binding protein and regulates growth factor-induced common postreceptor signal in vascular smooth muscle cell. *Circulation* 105: 2893–2898.
46. Kamada, Y., S. Tamura, S. Kiso, H. Matsumoto, Y. Saji, Y. Yoshida, K. Fukui, N. Maeda, H. Nishizawa, H. Nagaretani, et al. 2003. Enhanced carbon tetrachloride-induced liver fibrosis in mice lacking adiponectin. *Gastroenterology* 125: 1796–1807.
47. Ezure, T., and S. Amano. 2007. Adiponectin and leptin up-regulate extracellular matrix production by dermal fibroblasts. *Biofactors* 31: 229–236.
48. Fu, Y., N. Luo, R. L. Klein, and W. T. Garvey. 2005. Adiponectin promotes adipocyte differentiation, insulin sensitivity, and lipid accumulation. *J. Lipid Res.* 46: 1369–1379.
49. Kawai, K., A. Kageyama, T. Tsumano, S. Nishimoto, K. Fukuda, S. Yokoyama, T. Oguma, K. Fujita, S. Yoshimoto, A. Yanai, and M. Kakibuchi. 2008. Effects of adiponectin on growth and differentiation of human keratinocytes—implication of impaired wound healing in diabetes. *Biochem. Biophys. Res. Commun.* 374: 269–273.
50. Breitkreutz, D., H. J. Stark, P. Plein, M. Baur, and N. E. Fusenig. 1993. Differential modulation of epidermal keratinization in immortalized (HaCaT) and tumorigenic human skin keratinocytes (HaCaT-ras) by retinoic acid and extracellular Ca^{2+}. *Differentiation* 54: 201–217.
51. Tsuda, T., M. Tohyama, K. Yamasaki, Y. Shirakata, Y. Yahata, S. Tokumaru, K. Sayama, and K. Hashimoto. 2003. Lack of evidence for TARC/CCL17 production by normal human keratinocytes in vitro. *J. Dermatol. Sci.* 31: 37–42.
52. Hirose, H., T. Kawai, Y. Yamamoto, M. Taniyama, M. Tomita, K. Matsubara, Y. Okazaki, T. Ishii, Y. Oguma, I. Takei, and T. Saruta. 2002. Effects of pioglitazone on metabolic parameters, body fat distribution, and serum adiponectin levels in Japanese male patients with type 2 diabetes. *Metabolism* 51: 314–317.
53. Park, P. H., M. R. McMullen, H. Huang, V. Thakur, and L. E. Nagy. 2007. Short-term treatment of RAW264.7 macrophages with adiponectin increases tumor necrosis factor-α (TNF-α) expression via ERK1/2 activation and Egr-1 expression: role of TNF-α in adiponectin-stimulated interleukin-10 production. *J. Biol. Chem.* 282: 21695–21703.
54. Wijesekara, N., M. Krishnamurthy, A. Bhattacharjee, A. Suhail, G. Sweeney, and M. B. Wheeler. 2010. Adiponectin-induced ERK and Akt phosphorylation protects against pancreatic β cell apoptosis and increases insulin gene expression and secretion. *J. Biol. Chem.* 285: 33623–33631.
55. Turchi, L., A. A. Chassot, R. Rezzonico, K. Yeow, A. Loubat, B. Ferrua, G. Lenegrate, J. P. Ortonne, and G. Ponzio. 2002. Dynamic characterization of the molecular events during in vitro epidermal wound healing. *J. Invest. Dermatol.* 119: 56–63.
56. Yano, S., M. Komine, M. Fujimoto, H. Okochi, and K. Tamaki. 2004. Mechanical stretching in vitro regulates signal transduction pathways and cellular proliferation in human epidermal keratinocytes. *J. Invest. Dermatol.* 122: 783–790.
57. Xu, K. P., Y. Li, A. V. Ljubimov, and F. S. Yu. 2009. High glucose suppresses epidermal growth factor receptor/phosphatidylinositol 3-kinase/Akt signaling pathway and attenuates corneal epithelial wound healing. *Diabetes* 58: 1077–1085.
58. Zeigler, M. E., Y. Chi, T. Schmidt, and J. Varani. 1999. Role of ERK and JNK pathways in regulating cell motility and matrix metalloproteinase 9 production in growth factor-stimulated human epidermal keratinocytes. *J. Cell. Physiol.* 180: 271–284.

Diabetologia (2012) 55:3382–3391
DOI 10.1007/s00125-012-2703-1

ARTICLE

Protection from non-alcoholic steatohepatitis and liver tumourigenesis in high fat-fed insulin receptor substrate-1-knockout mice despite insulin resistance

A. Nakamura · K. Tajima · K. Zolzaya · K. Sato · R. Inoue · M. Yoneda · K. Fujita · Y. Nozaki · K. C. Kubota · H. Haga · N. Kubota · Y. Nagashima · A. Nakajima · S. Maeda · T. Kadowaki · Y. Terauchi

Received: 28 May 2012 / Accepted: 27 July 2012 / Published online: 7 September 2012

Abstract
Aims/hypothesis Epidemiological studies have revealed that obesity and diabetes mellitus are independent risk factors for the development of non-alcoholic steatohepatitis (NASH) and hepatocellular carcinoma. However, the debate continues on whether insulin resistance as such is directly associated with NASH and liver tumourigenesis. Here, we investigated the incidence of NASH and liver tumourigenesis in *Irs1*$^{-/-}$ mice subjected to a long-term high-fat (HF) diet. Our hypothesis was that hepatic steatosis, rather than insulin resistance may be related to the pathophysiology of these conditions.
Methods Mice (8 weeks old, C57Bl/6J) were given free access to standard chow (SC) or an HF diet. The development of NASH and liver tumourigenesis was evaluated after mice had been on the above-mentioned diets for 60 weeks. Similarly, *Irs1*$^{-/-}$ mice were also subjected to an HF diet for 60 weeks.
Results Long-term HF diet loading, which causes obesity and insulin resistance, was sufficient to induce NASH and liver tumourigenesis in the C57Bl/6J mice. Obesity and insulin resistance were reduced by switching mice from the HF diet to SC, which also protected these mice against the development of NASH and liver tumourigenesis. However, compared with wild-type mice fed the HF diet, *Irs1*$^{-/-}$ mice fed the HF diet were dramatically protected against NASH and liver tumourigenesis despite the presence of severe insulin resistance and marked postprandial hyperglycaemia.
Conclusions/interpretation IRS-1 inhibition might protect against HF diet-induced NASH and liver tumourigenesis, despite the presence of insulin resistance.

Keywords High-fat diet · Insulin receptor substrate-1 · Insulin resistance · Liver tumourigenesis · Non-alcoholic steatohepatitis

Abbreviations

ALT	Alanine aminotransferase
HCC	Hepatocellular carcinoma
H&E	Haematoxylin and eosin
HF	High-fat
HOMA-IR	HOMA of insulin resistance

A. Nakamura and K. Tajima contributed equally to this work.

Electronic supplementary material The online version of this article (doi:10.1007/s00125-012-2703-1) contains peer-reviewed but unedited supplementary material, which is available to authorised users.

A. Nakamura · K. Tajima · K. Zolzaya · K. Sato · R. Inoue · Y. Terauchi (✉)
Department of Endocrinology and Metabolism, Graduate School of Medicine, Yokohama City University, 3-9 Fukuura, Kanazawa-ku, Yokohama 236-0004, Japan
e-mail: terauchi-tky@umin.ac.jp

M. Yoneda · K. Fujita · Y. Nozaki · A. Nakajima · S. Maeda
Division of Gastroenterology, Graduate School of Medicine, Yokohama City University, Yokohama, Japan

K. C. Kubota · H. Haga
Department of Surgical Pathology, Hokkaido University Hospital, Sapporo, Japan

N. Kubota · T. Kadowaki
Department of Diabetes and Metabolic Diseases, Graduate School of Medicine, University of Tokyo, Tokyo, Japan

Y. Nagashima
Department of Molecular Pathology, Graduate School of Medicine, Yokohama City University, Yokohama, Japan

NAFLD	Non-alcoholic fatty liver disease
NASH	Non-alcoholic steatohepatitis
PI3K	Phosphoinositide 3-kinase
SC	Standard chow

Introduction

The prevalence of obesity and diabetes has been increasing globally over the past 30 years [1, 2]. These diseases not only increase cardiovascular risk, but also cancer risk and mortality rates [3, 4]. Especially, hepatocellular carcinoma (HCC), the fifth most common cancer and the third leading cause of cancer death worldwide [5], accounts for the largest increase in cancer and mortality risk in individuals with obesity or diabetes [3, 4]. Certain cases of HCC may be associated with infection with hepatitis B or C virus, or chronic alcohol use. However, an increasing number of cases are associated with non-alcoholic fatty liver disease (NAFLD). NAFLD encompasses a clinicopathological spectrum of diseases ranging from isolated hepatic steatosis to non-alcoholic steatohepatitis (NASH), the more aggressive form of fatty liver disease, which may progress to cirrhosis and cirrhosis-related complications including HCC. The prevalence of NAFLD, including NASH, is also increasing in parallel with the growing obesity and diabetes epidemics [5].

Although the causal relationships between obesity or diabetes, and NASH or liver tumourigenesis have not yet been clearly elucidated, it is assumed that the insulin resistance associated with obesity and diabetes is involved in the development of hepatic steatosis and inflammation in the liver, which may progress to NASH and liver tumourigenesis [5]. Indeed, long-term high-fat (HF) diet loading, which can induce obesity and insulin resistance, was sufficient to induce NASH and liver tumourigenesis in C57Bl/6J mice [6–8]. Thus, this experimental model supports the above-mentioned concept.

IRS-1 and -2 exhibit a high structural homology, are abundantly produced in the liver and are thought to be responsible for transmitting insulin signalling from the insulin receptor to intracellular effectors in the regulation of glucose and lipid homeostasis [9, 10]. Insulin receptor signalling can be almost exclusively mediated by IRS-1 and IRS-2 in the liver [10]; indeed, a dominant role of IRS-1 has been observed during nutrient excess [11]. Moreover, HF diet-fed liver-specific *Irs1*$^{-/-}$ mice displayed severe insulin resistance, but not hepatic steatosis [11]. Also, mice with acyl-CoA:diacylglycerol acyltransferase (DGAT)2 overabundance in the liver reportedly developed hepatic steatosis without abnormal plasma glucose and insulin levels [12], while liver-specific phosphoinositide 3-kinase (PI3K) p110α-knockout (*Pik3ca*$^{-/-}$) mice fed an HF diet were protected against hepatic steatosis without ameliorating HF diet-induced glucose intolerance [13]. Mice with genetic defects or targeted overexpression, such as hepatocyte-specific *Pten*-knockout mice and *Pik3ca* transgenic mice [14, 15], have been reported to be models of NAFLD and liver tumourigenesis, but might not reflect the natural aetiology of NASH and liver tumourigenesis in human participants. Rather, insulin sensitivity was improved in hepatocyte-specific *Pten*-knockout mice, compared with wild-type mice [14], and *Pik3ca* transgenic mice exhibited better glucose tolerance than wild-type mice [15]. Therefore, liver steatosis can occur independently of insulin resistance.

In the present study, we investigated the effect of a long-term HF diet on the development of NASH and liver tumourigenesis using C57Bl/6J male mice. Next, we performed similar experiments in which the HF diet was switched to a standard chow (SC) diet to clarify the effect of improved insulin resistance on the development of these diseases. We also investigated the incidence of NASH and liver tumourigenesis in *Irs1*$^{-/-}$ mice subjected to a long-term HF diet. The hypothesis behind this part of the study was that hepatic steatosis, rather than insulin resistance, may be related to the pathophysiology of these conditions.

Methods

Animals Mice (*Irs1*$^{-/-}$) were generated as described elsewhere [16]. We backcrossed these mice with C57Bl/6J mice more than nine times. Male littermates derived from the intercrosses were fed an SC diet until 8 weeks of age and then had free access to the SC diet or an HF diet. In the dietary switch experiment, 8-week-old C57Bl/6J male mice were subjected to the HF diet for 30 weeks and then switched to the SC diet for the next 30 weeks; these mice were then compared with mice from the same genetic background that had received the HF diet for the entire 60 weeks. The mice were housed under a 12 h light–dark cycle. The animals were maintained according to standard animal care procedures based on institutional guidelines. These experiments involving animals were approved by the local Ethics Committee of the Yokohama City University.

Diet protocol We used an SC diet (MF; Oriental Yeast, Tokyo, Japan) and an HF diet (High-Fat Diet 32; Clea Japan, Tokyo, Japan). The composition of each of these diets is shown in electronic supplementary material (ESM) Table 1. The fatty acid composition of the HF diet consisted of 22% (wt/wt) saturated fatty acid (12.6% palmitic acid, 7.5% stearic acid) and 77% (wt/wt) unsaturated fatty acid (64.3% oleic acid, 10.2% linoleic acid).

Measurement of biochemical variables Blood glucose levels were measured using a portable glucose meter and Glutest Neo (Sanwa Chemical, Nagoya, Japan). Insulin levels were determined using an insulin ELISA kit (Morinaga, Yokohama,

Japan). Plasma alanine aminotransferase (ALT) levels were assayed using an enzymatic method (Wako Pure Chemical, Osaka, Japan). The plasma levels of total adiponectin and leptin were measured using ELISAs (Otsuka Pharmaceutical, Tokyo, Japan, and Morinaga, respectively). The triacylglycerol content of the liver was determined as described elsewhere [10]. HOMA of insulin resistance (HOMA-IR) was calculated by using the formula [fasting insulin (mU/l)×fasting plasma glucose (mmol/l)] / 22.5. When insulin is expressed in SI units as pmol/l, the constant changes to 156.26.

Glucose tolerance test Mice were denied access to food for more than 16 h before the study and then orally loaded with glucose at 1.5 mg/g body weight. Blood samples were collected before, and at 15, 30, 60 and 120 min after glucose loading.

Insulin tolerance test The insulin tolerance test was performed under non-fasting conditions. Insulin was injected intraperitoneally, and blood samples were collected before, and at 30, 60, 90 and 120 min after the injection.

Histopathological evaluation Liver samples were immersion-fixed overnight in 10% formalin (vol./vol.) at 4°C. The tissues were then routinely processed for paraffin embedding, and 5 μm sections mounted on glass slides were processed for haematoxylin and eosin (H&E) staining. The presence of collagen, which can be used as an index of fibrosis in lesions, was examined using Masson trichrome-stained preparations.

Liver histology and scoring system All the histopathological findings were scored by experienced pathologists, who were unaware of the genetic backgrounds and diets of the mice. The histological features were grouped into three broad categories: steatosis, inflammation and fibrosis. The scoring system used for the evaluation is detailed in ESM Table 2.

RNA preparation and real-time quantitative PCR Total RNA was prepared from portions of the liver using a reagent (Isogen; NipponGene, Tokyo, Japan), according to the manufacturer's instructions, and these samples were used as the starting material for cDNA preparations. cDNA was synthesised using reagents (TaqMan Reverse Transcription; Applied Biosystems, Foster City, CA, USA), followed by TaqMan quantitative PCR (50°C for 2 min and 95°C for 10 min, followed by 40 cycles at 95°C for 15 s and at 60°C for 1 min), performed on a PCR instrument (ABI Prism 7500; Applied Biosystems) to amplify the following genes: *Pparg*, *Srebp1c* (also known as *Srebf1*), *Fas*, *Scd1*, *Ppara*, *Cpt1* (also known as *Cpt1a*), *Mcad* (also known as *Acadm*), *Tnfa* (also known as *Tnf*), *Mcp1* (also known as *Ccl2*), *p22phox* (also known as *Cyba*), *gp91phox* (also known as *Cybb*), *p47phox* (also known as *Ncf1*) and *Irs2*. The relative expression levels were then compared after normalisation to the expression of beta-actin.

Statistical analysis Results are expressed as means ± SEM (*n*). Differences between two groups were analysed for statistical significance using Student's *t* test. Individual comparisons among four groups were performed using an ANOVA followed by Fisher's protected least significant difference post-hoc test. Also, individual comparisons between two time points and two groups were performed using a two-way ANOVA. A value of $p<0.05$ was considered statistically significant.

Results

Effects of long-term HF diet on metabolic changes in C57Bl/6J mice First, we tested the effect of long-term HF diet loading on the development of NASH and liver tumourigenesis in C57Bl/6J male (wild-type) mice. After 30 and 60 weeks on the HF diet, this mouse model showed higher body weights, fasting blood glucose levels, liver weights and plasma ALT levels than mice fed SC, but the plasma ALT levels were not significantly higher, presumably because of an interaction effect (Fig. 1a–d). The triacylglycerol content of the liver tended to be higher in wild-type mice after 30, but not after 60 weeks on the HF diet, compared with that in mice fed the SC diet (Fig. 1e). The glucose-lowering effect of insulin was impaired in this mouse model when fed the HF diet, compared with that in the same mouse model on the SC diet (Fig. 1f). Thus, the long-term administration of an HF diet induced obesity and insulin resistance in C57Bl/6J male mice. Furthermore, fasting insulin levels, HOMA of insulin resistance (HOMA-IR) and leptin levels were significantly higher, while plasma adiponectin levels were significantly lower in animals fed the HF diet than in those fed the SC diet (Fig. 1g–j), consistent with the results of previous reports [17, 18].

Effects of long-term HF diet on the risk of occurrence of NASH and liver tumourigenesis in C57Bl/6J mice Livers from wild-type mice fed the HF diet for 60 weeks were enlarged, compared with those in animals fed the SC diet for the same duration (Fig. 2a). Whereas wild-type mice on the SC diet had an almost normal liver histology (Fig. 2b, e), those fed the HF diet had typical features of NASH (Fig. 2c) at various stages of progression in the liver, including portal inflammation (Fig. 2d) and blue wave-like bands of fibrotic tissue in portal lesions (Fig. 2f, g). Scoring of the pathological findings showed significant increases for liver steatosis, inflammation and fibrosis in wild-type mice fed the HF diet, compared with scores in their counterparts on the SC diet (Fig. 2h). The expression of lipogenic genes, such as *Fas* and *Scd1*, after 30 weeks (Fig. 2i), and of genes encoding

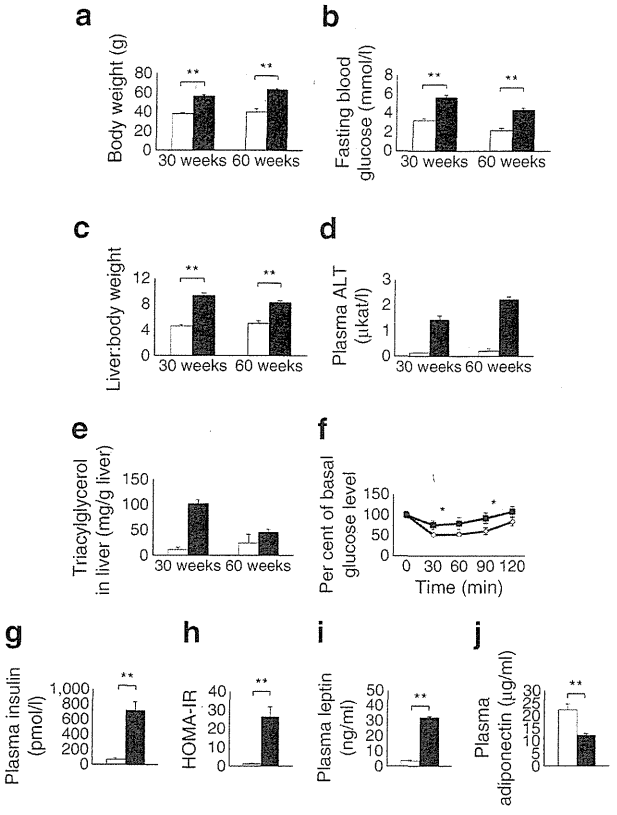

Fig. 1 Effects of a long-term HF diet on metabolic changes in C57Bl/6J mice. (**a**) Body weight, (**b**) fasting blood glucose, (**c**) ratio of liver: body weight, (**d**) plasma ALT and (**e**) triacylglycerol content of liver in mice fed the SC (white bars) or HF (black bars) diet for 30 or 60 weeks (n=8–24). (**f**) Insulin tolerance test in mice fed the SC (white diamonds) or HF (black squares) diet for 60 weeks (n=6). (**g**) Plasma fasting insulin levels, (**h**) HOMA-IR calculated from fasting blood glucose and insulin levels, (**i**) leptin levels and (**j**) total adiponectin levels in mice fed the SC or HF diet for 30 weeks (n=10–11). Values are mean ± SEM; *p<0.05 and **p<0.01

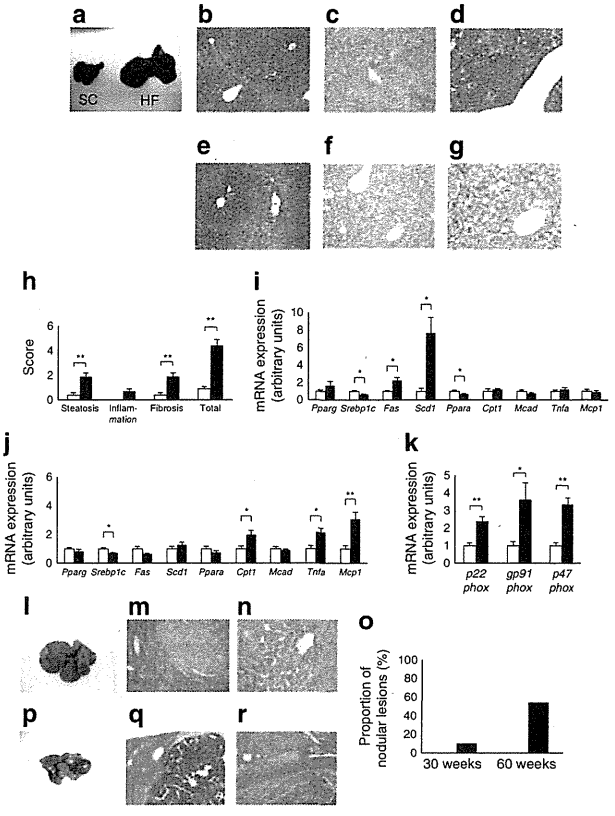

Fig. 2 Effects of a long-term HF diet on the risk of NASH and liver tumourigenesis in C57Bl/6J mice. (**a**) Macroscopic findings after 60 weeks. (**b**, **e**) Histopathological findings in the livers of mice fed the SC or HF (**c**, **d**, **f**, **g**) diets, as assessed using H&E- (**b**–**d**) and Masson trichrome (**e**–**g**)-stained sections. (**h**) The NASH/NAFLD Clinical Research Network scoring system definition and scores [32] for mice fed the SC (white bars) or HF (black bars) diet (n=9). (**i**) mRNA expression of lipogenic and inflammatory cytokine-related genes as listed after 30 and 60 (**j**) weeks, and (**k**) of genes encoding the reduced-form NADPH oxidase complex after 60 weeks in mice fed the SC or HF diet (n=5–6). (**l**) Macroscopic and (**m**, **n**) histopathological findings in sections containing liver tumours, as assessed using H&E-stained sections from mice fed the HF diet for 60 weeks. (**o**) Proportion of hepatic nodular lesions in mice fed the SC or HF diet (n=8–24). (**p**) Macroscopic and (**q**, **r**) histopathological features as assessed using H&E-stained sections of hepatic tumours from mice fed the HF diet for 80 weeks. Values are mean ± SEM; *p<0.05 and **p<0.01

inflammatory cytokines, such as *Tnfa* and *Mcp1*, after 60 weeks (Fig. 2j) was significantly increased in wild-type mice fed the HF diet, compared with that in animals fed the SC diet. Furthermore, the expression of genes encoding the reduced-form NADPH oxidase complex was coordinately elevated after 60 weeks in mice fed the HF diet, compared with findings in animals fed the SC diet (Fig. 2k). These results reflect the natural course of NASH: in other words, healthy liver becomes steatotic, followed by an inflammatory process caused by cytokines and oxidative stress, which results in hepatocellular degeneration and fibrosis. Moreover, tumours of various diameters were frequently observed on the liver surface in the HF group (Fig. 2l). Pathologically, these tumours were dysplastic nodules, adenomas or well-differentiated carcinomas (Fig. 2m, n), consistent with the findings of previous reports [6, 7]. These nodular lesions were observed on the liver surface in 10% of animals after 30 weeks and in 54% of animals after 60 weeks of administration of the HF diet in wild-type mice. In contrast, no such nodular lesions were detected in mice fed the SC diet (Fig. 2o). Interestingly, HCCs, which are characterised by disrupted normal liver architecture and intravascular tumour embolism, were found in certain mice after 80 weeks on the HF diet (Fig. 2p–r). As a point of reference, no increase in the phosphorylation levels of c-Jun N-terminal kinase (JNK), extracellular signal-regulated kinase (ERK) or p38 were noted in wild-type mice fed the HF diet, compared with the levels in mice fed the SC diet (data not shown). These results indicate that the long-term HF diet loading was sufficient to induce NASH and liver tumourigenesis in wild-type mice.

Switching from the HF to the SC diet: effects on metabolic changes in C57Bl/6J mice Next, to evaluate the effects of nutrients on fat distribution within the body, the degree of insulin resistance, and the risk of NASH and liver tumourigenesis, we compared C57Bl/6J male mice that were fed the HF diet for 30 weeks, followed by 30 weeks on the SC diet, with mice from the same genetic background that were fed the HF diet for the entire 60 weeks. The mice that were switched from the HF diet to the SC diet showed a significantly lower body weight and visceral fat weight than the animals that were fed the HF diet for the entire 60 weeks, although no differences in fed-state blood glucose levels were observed between the two groups (Fig. 3a–d). The diet switch improved the degree of hyperinsulinaemia and insulin resistance, as evidenced by fasting insulin levels, HOMA-IR and insulin tolerance test results (Fig. 3e, f, ESM Fig. 1). The diet switch was also associated with a decrease in liver weight, plasma ALT levels and liver triacylglycerol content, although the difference for the latter was not statistically significant (Fig. 3g–j).

Switching from the HF to the SC diet: effects on the incidence of NASH and liver tumourigenesis in C57Bl/6J mice Compared with the findings for mice that continued the HF diet for the entire 60 weeks, findings for mice that were switched from the HF to the SC diet showed an almost normal liver histology (Fig. 4a, b), with significantly decreased pathological scores for NASH (Fig. 4c). Also, the expression of genes encoding inflammatory cytokines such as *Tnfa* and *Mcp1*, and the reduced-form NADPH oxidase complex decreased significantly in the group that switched diets (Fig. 4d, e). The proportion of nodular lesions was also significantly decreased by the dietary switch (Fig. 4f). These findings suggest that the correction of nutrient conditions improved obesity and the related insulin resistance, and protected the animals against HF diet-induced NASH and liver tumourigenesis.

Effects of long-term HF diet on metabolic changes in Irs1$^{-/-}$ mice To evaluate the effect of hepatic steatosis on HF diet-induced NASH and liver tumourigenesis, we used *Irs1*$^{-/-}$ male mice, which exhibit postnatal growth retardation and insulin resistance, but have normal glucose tolerance because of compensatory beta cell hyperplasia [19–21]. As expected, the body weight of *Irs1*$^{-/-}$ mice was about two thirds that of wild-type mice in the SC and HF diet groups (Fig. 5a). However, fed-state blood glucose levels were increased in *Irs1*$^{-/-}$ mice, compared with those in wild-type mice, after 6 weeks on the HF diet, although no differences in fed-state glucose levels were observed between wild-type and *Irs1*$^{-/-}$ mice fed the SC diet (Fig. 5b). Interestingly, the liver weight, plasma ALT levels and triacylglycerol content of the liver were significantly higher in wild-type mice fed the HF diet than in the other groups of mice (Fig. 5c–e). Moreover, although wild-type

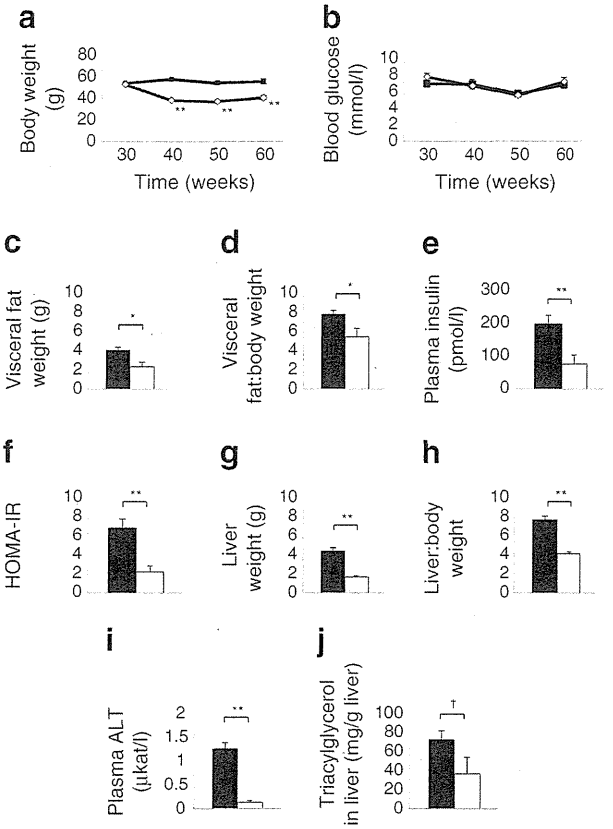

Fig. 3 Effects of the switch from the HF to the SC diet on metabolic changes in C57Bl/6J mice. The mice were fed the HF diet for 30 weeks, followed by the SC diet for 30 weeks. They were then compared with mice fed the HF diet for 60 weeks. (**a**) Changes in body weight and (**b**) fed-state blood glucose levels in the HF diet alone (black squares) and HF + SC diet (white diamonds) groups (n=10). (**c**) Visceral fat weight and (**d**) the ratio of visceral fat weight to body weight in the HF diet alone (black bars) and the HF + SC diet (white bars) groups (n=5). (**e**) Plasma fasting insulin, (**f**) HOMA-IR, (**g**) liver weight, (**h**) ratio of liver to body weight, (**i**) plasma ALT and (**j**) triacylglycerol content of the liver in the two groups of mice (n=10). Values are mean ± SEM; *p< 0.05 and **p<0.01; †p=0.08

mice fed the HF diet demonstrated the typical features of hepatic steatosis, the other three groups showed an almost normal liver histology (Fig. 5f–i). These results indicate that the disruption of IRS-1 protected against HF diet-induced hepatic steatosis.

Based on these results, we next compared the effects of long-term HF diet loading on metabolic changes in *Irs1*$^{-/-}$ mice relative to those in wild-type mice. Although the body weight of *Irs1*$^{-/-}$ mice was about two thirds that of wild-type mice and the visceral fat weight in the former was also lower (*Irs1*$^{-/-}$ mice 2.3±0.1 g vs wild-type 3.9±0.1 g), no difference in the ratio of visceral weight to body weight was observed between the two groups (Fig. 6a–c). The insulin and oral glucose tolerance tests revealed that *Irs1*$^{-/-}$ mice

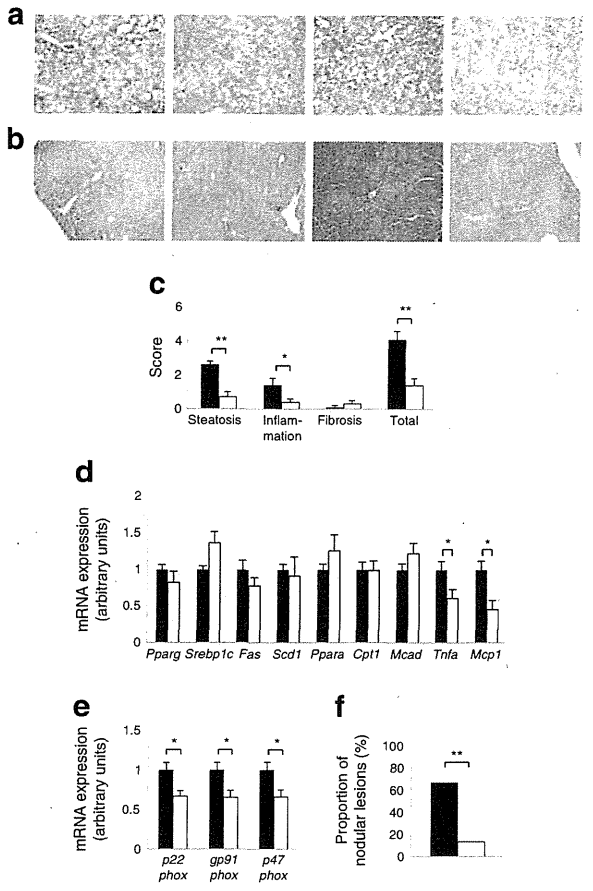

Fig. 4 Effects of switching from the HF to the SC diet on the incidence of NASH and liver tumourigenesis in C57Bl/6J mice. The mice were fed the HF diet for 30 weeks, followed by the SC diet for 30 weeks. They were then compared with mice fed the HF diet for 60 weeks. (**a**) Histopathological findings of NASH in the livers from the HF diet alone group and (**b**) the HF + SC diet group, as observed using H&E-stained sections (n=4). (**c**) NASH/NAFLD Clinical Research Network scoring system definitions and scores [32] for the HF diet alone (black bars) and the HF + SC diet (white bars) groups of mice (n=9–10). (**d**) mRNA expression of lipogenic and inflammatory cytokine-related genes, and (**e**) of genes encoding the reduced-form NADPH oxidase complex in the two groups of mice (n=4–6). (**f**) Proportion of hepatic nodular lesions in the two groups of mice (n=15). Values are mean ± SEM; $^{*}p<0.05$ and $^{**}p<0.01$

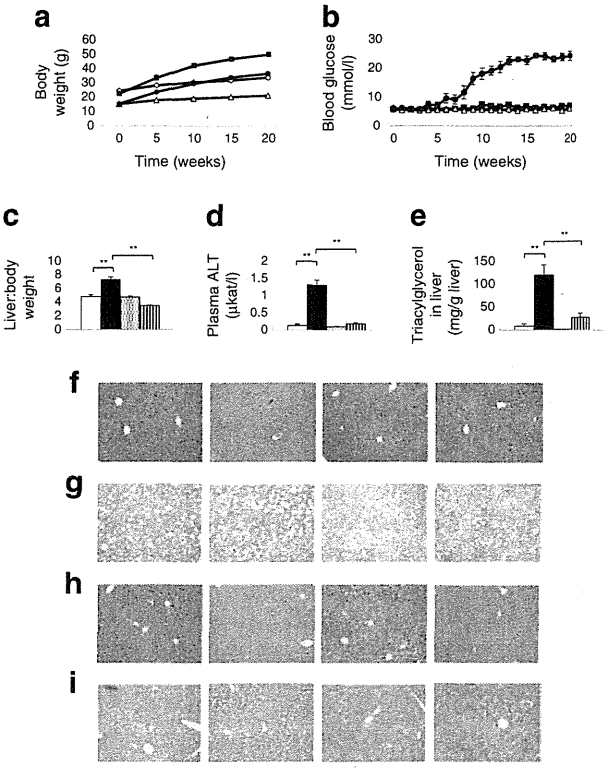

Fig. 5 Effects of an HF diet on liver steatosis in $Irs1^{-/-}$ mice. (**a**) Changes in the body weight and (**b**) fed-state blood glucose levels in wild-type and $Irs1^{-/-}$ mice fed the SC or HF diet (white diamonds, wild-type SC; black squares, wild-type HF; white triangles, $Irs1^{-/-}$ SC; black circles, $Irs1^{-/-}$ HF) (n=7–11). (**c**) Ratio of liver weight to body weight, (**d**) plasma ALT and (**e**) triacylglycerol content of the liver in mice as above (**a**, **b**) at 20 weeks of respective diet (white bars, wild-type SC; black bars, wild-type HF; dotted bars, $Irs1^{-/-}$ SC; striped bars, $Irs1^{-/-}$ HF) (n=5–10). (**f**) Histopathological findings in the livers of wild-type SC-, (**g**) wild-type HF-, (**h**) $Irs1^{-/-}$ SC- and (**i**) $Irs1^{-/-}$ HF-fed mice, as assessed using H&E-stained sections (n=4). Values are mean ± SEM; $^{**}p<0.01$

fed the HF diet had severe insulin resistance and marked postprandial hyperglycaemia compared with wild-type mice on the same diet (Fig. 6d, e). Also, their fasting insulin levels and HOMA-IR values were significantly higher than in wild-type mice (Fig. 6f, g). Moreover, the liver weight, plasma ALT levels and triacylglycerol content of the liver were significantly lower in $Irs1^{-/-}$ mice than in wild-type mice fed the HF diet (Fig. 6a, h–j). Although no difference in plasma leptin levels was seen, adiponectin levels were significantly higher in $Irs1^{-/-}$ mice (Fig. 6k, l).

Effects of long-term HF diet on the incidence of NASH and liver tumourigenesis in $Irs1^{-/-}$ mice Apparently, $Irs1^{-/-}$ mice fed the HF diet showed an almost normal liver histology (Fig. 7a–d), while pathological scores for NASH were significantly lower in $Irs1^{-/-}$ mice (Fig. 7e). Also, the expression of lipogenic genes such as *Fas* and *Scd1* at 30 weeks, and of genes encoding inflammatory cytokines and the reduced-form NADPH oxidase complex at 60 weeks were significantly decreased in $Irs1^{-/-}$ mice on the HF diet, compared with wild-type mice fed the same diet (Fig. 7f–h). Moreover, the proportion of nodular lesions was significantly lower in $Irs1^{-/-}$ mice fed the HF diet than in wild-type mice on the same diet (Fig. 7i). These results indicate that the disruption of IRS-1 protected against HF diet-induced NASH and liver tumourigenesis, despite being associated with severe hyperglycaemia and insulin resistance.

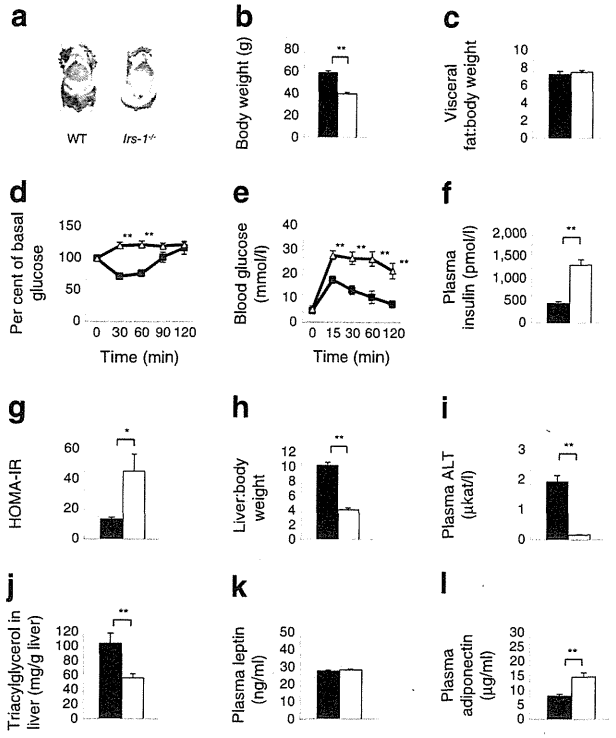

Fig. 6 Effects of a long-term HF diet on metabolic changes in *Irs1*$^{-/-}$ mice. (**a**) Macroscopic observation in wild-type (WT) and *Irs1*$^{-/-}$ mice fed the HF diet. (**b**) Body weight and (**c**) ratio of visceral weight to body weight in wild-type (black bars) and *Irs1*$^{-/-}$ (white bars) mice fed the HF diet for 30 weeks (n=4–10). (**d**) Insulin and (**e**) oral glucose tolerance tests in wild-type (black squares) and *Irs1*$^{-/-}$ (white triangles) mice fed the HF diet for 30 weeks (n=8–10). (**f**) Plasma fasting insulin, (**g**) HOMA-IR, (**h**) ratio of liver weight to body weight, (**i**) plasma ALT, (**j**) hepatic triacylglycerol content, (**k**) plasma leptin levels and (**l**) plasma total adiponectin levels in wild-type and *Irs1*$^{-/-}$ mice fed the HF diet for 30 weeks (n=6–10). Values are mean ± SEM; *p<0.05 and **p<0.01

Discussion

In the present study, we showed that long-term HF diet loading, which causes obesity and peripheral insulin resistance, was sufficient to induce NASH and liver tumourigenesis in C57Bl/6J mice, and that the reduction of obesity and peripheral insulin resistance by switching from the HF to an SC diet protected animals against the development of NASH and liver tumourigenesis. More importantly, the results of our study indicate that *Irs1*$^{-/-}$ mice fed the HF diet were dramatically protected against NASH and liver tumourigenesis, despite having severe insulin resistance and marked postprandial hyperglycaemia. These results are not consistent with the prevalent notion that the insulin resistance associated with obesity and diabetes is involved in the development of hepatic steatosis and inflammation in the liver, which may progress to NASH and liver tumourigenesis [5].

How can these results be explained? One explanation is the concept of selective or partial insulin resistance [22]. Thus humans with insulin resistance caused by inherited mutations in the insulin receptor and mice with a liver-specific deletion of the insulin receptor have hyperglycaemia and hyperinsulinaemia, but are both protected against hepatic steatosis and hypertriacylglycerolaemia [23, 24]. This finding is consistent with the idea that not all signals are blunted in classical insulin-resistant states; instead, some signals are preserved, particularly those related to hepatic steatosis.

Insulin receptor signalling can be almost exclusively mediated by IRS-1 and IRS-2 in the liver, with IRS-2 mainly functioning during fasting and immediately after re-feeding, while IRS-1 functions primarily after re-feeding [10]. In our results in wild-type mice, *Irs2* levels were significantly decreased in the HF diet group, compared with those in the SC diet group, under fasting conditions, while levels of *Irs1* in the HF diet group were similar to those in the SC diet group under re-feeding conditions (ESM Fig. 2). Insulin signalling might be decreased mainly under fasting conditions in the HF diet group, as the hyperinsulinaemia associated with an HF diet may suppress IRS-2 production [25]. In this case, HF diet feeding might place the mice in a chronic postprandial state that preferentially inactivates IRS-2, with persistent IRS-1 signalling possibly promoting lipogenesis and leading to hepatic steatosis, since IRS-1 has been proposed to be the dominant regulator of expression of the hepatic genes controlling lipogenesis [11]. In contrast, hepatic insulin signalling in *Irs1*$^{-/-}$ mice fed the HF diet was impaired, since IRS-1 was absent and IRS-2 signalling was suppressed by the hyperinsulinaemia associated with the HF diet. Thus, the pathophysiological features in *Irs1*$^{-/-}$ mice fed the HF diet might be similar to those in liver-specific *Irs1*/*Irs2* double-knockout mice and in liver-specific insulin receptor knockout mice [11, 24]. A similar situation is seen with the liver-specific loss-of-function of the p110α subunit of PI3K [13] or of Akt [26]. Since the IRS proteins lie between these steps [27], these previous studies using mouse models with genetic engineering of genes encoding the insulin receptor, IRS, PI3K and Akt are consistent with the phenotype of the *Irs1*$^{-/-}$ mice fed the HF diet in our study.

Importantly, the mice in the present study, unlike liver-specific knockout mice, had impaired IRS-1 functions in all their tissues. It thus remains unclear whether the protection against NASH and liver tumourigenesis is due to a global loss of insulin signalling or a liver-specific loss. Unfortunately, the current data do not answer this question. However, we assumed that the protection might be due to a liver-autonomous effect, since liver-specific *Irs1*$^{-/-}$ mice fed an HF diet, but not liver-specific *Irs2*$^{-/-}$ mice fed an HF diet were reportedly protected from hepatic steatosis [11] and the steatotic host microenvironment probably sets the stage for tumour development, even during the initially reversible and treatable stages of fatty liver disease [7]. Therefore, this

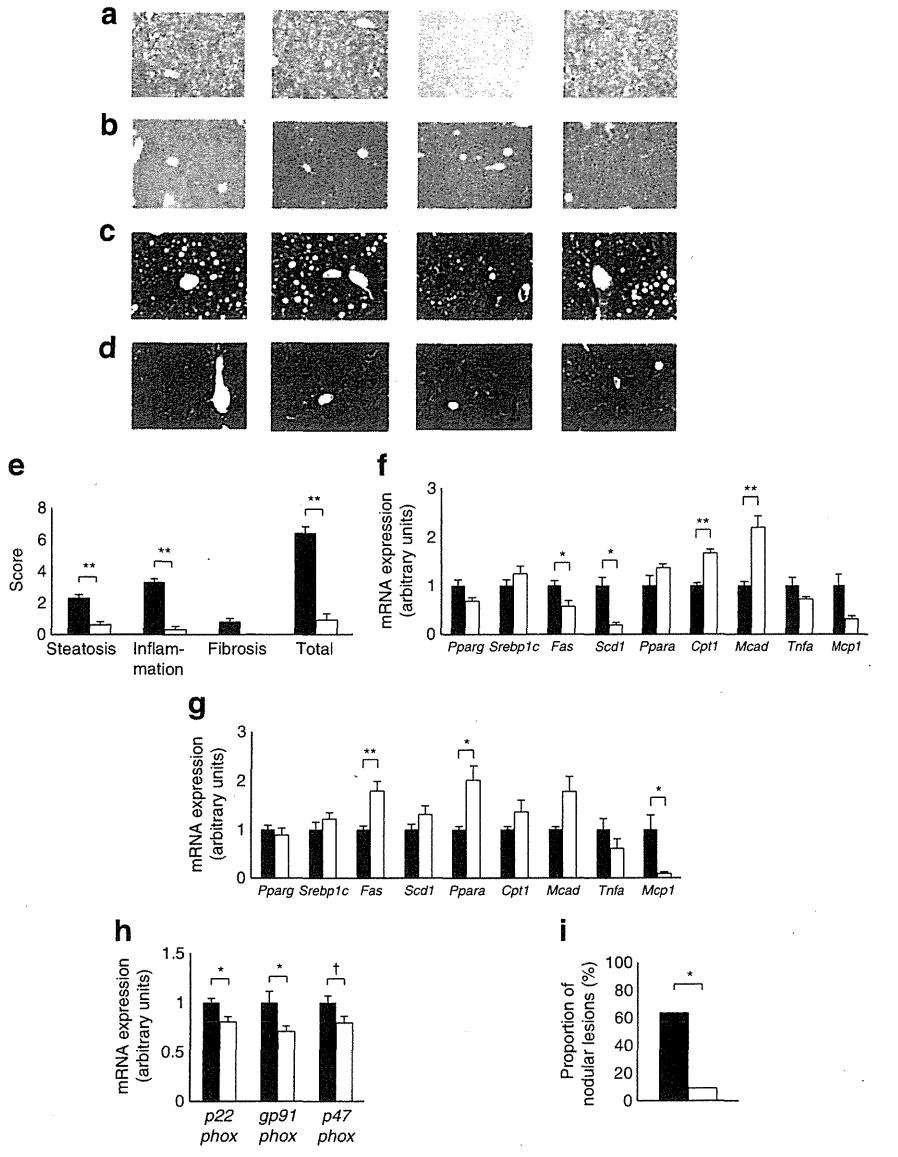

Fig. 7 Effects of a long-term HF diet on the incidence of NASH and liver tumourigenesis in *Irs1*$^{-/-}$ mice. (**a**) Histopathological features of the livers from wild-type and (**b**) *Irs1*$^{-/-}$ mice fed the HF diet for 60 weeks, as assessed using H&E-stained sections (n=4). (**c**) Histopathological features of the livers from wild-type and (**d**) *Irs1*$^{-/-}$ mice fed the HF diet for 60 weeks, as assessed using Masson trichrome-stained sections (n=4). (**e**) NASH/NAFLD Clinical Research Network scoring system definitions and scores [32] for wild-type (black bars) and *Irs1*$^{-/-}$ (white bars) mice fed the HF diet for 60 weeks (n=9). (**f**) mRNA expression of lipogenic and inflammatory cytokine-related genes after 30 and (**g**) 60 weeks on the HF diet, and (**h**) of genes encoding the reduced-form NADPH oxidase complex after 60 weeks on the HF diet in wild-type and *Irs1*$^{-/-}$ mice (n=4–6). (**i**) Proportion of hepatic nodular lesions in wild-type and *Irs1*$^{-/-}$ mice fed the HF diet for 60 weeks (n=11). Values are mean ± SEM; $^{*}p<0.05$ and $^{**}p<0.01$; $^{\dagger}p=0.05$

hypothesis should be further examined using liver-specific *Irs1*$^{-/-}$ and *Irs2*$^{-/-}$ mice [10] in the future.

Another question that remains unclear is whether the contribution or compensation of IRS-2 signalling plays a role in the above-mentioned protective effect. Our data show that *Irs2* expression in *Irs1*$^{-/-}$ mice on the HF diet was significantly higher than in wild-type mice fed the HF diet. However, levels were significantly lower than those in wild-type mice fed the SC diet. Moreover, the basal and insulin-stimulated phosphorylation of Akt in *Irs1*$^{-/-}$ mice on the HF diet was lower than in wild-type mice fed the HF diet (data not shown). These results suggest that IRS-2 may not fully compensate for the loss of IRS-1 in *Irs1*$^{-/-}$ mice on an HF diet. We therefore assumed that the contribution of residual IRS-2 signalling was limited to the livers of *Irs1*$^{-/-}$ mice on the HF diet.

What is the relevance of the present results to the clinical management of humans with diabetes? Therapeutic targeting of IRS-1 may not be advisable, since *IRS1* is an insulin resistance gene in humans [28] and our results suggest that blocking IRS-1-mediated signalling exacerbated glucose tolerance, even though it was able to protect against NASH and liver tumourigenesis. Epidemiological evidence suggests that people with diabetes have significantly higher risks of many forms of cancer [29]. Recently, a meta-analysis of several studies showed that liver cancer is more common in patients with diabetes [30].

Johnson et al commented that the accumulation of experimental and epidemiological evidence is more consistent with the hyperinsulinaemia hypothesis and less so with the hyperglycaemia hypothesis [31] with regard to the increased risk of cancer in patients with diabetes. Here, we showed that the reduction of obesity and hyperinsulinaemia by switching from an HF to an SC diet protected mice against the development of NASH and liver tumourigenesis without changing blood glucose levels. These results support the hyperinsulinaemia hypothesis. How can our results for *Irs1*$^{-/-}$ mice fed an HF diet be explained? We assumed that the protection against NASH and tumour development in *Irs1*$^{-/-}$ mice fed the HF diet was caused by the downregulation of IRS-1-mediated insulin action in the liver, despite systemic hyperinsulinaemia. As described above, the hyperinsulinaemia associated with an HF diet suppresses IRS-2 production, and persistent IRS-1 signalling promotes lipogenesis and hepatic steatosis. Thus, when mice were fed the HF diet, the wild-type mice developed hepatic steatosis, but the *Irs1*$^{-/-}$ mice were protected against the development of NASH and liver tumourigenesis, despite the presence of hyperinsulinaemia. Thus, these results for *Irs1*$^{-/-}$ mice fed an HF diet are consistent with the above-mentioned hyperinsulinaemia hypothesis. Therefore, the prevention of hyperinsulinaemia using glucose-lowering agents such as metformin and thiazolidinedione could not only protect against diabetes, but also against liver tumourigenesis. The effects of metformin on NASH and liver tumourigenesis in this mouse model are now under investigation.

In conclusion, long-term HF diet loading was sufficient to induce NASH and liver tumourigenesis in C57Bl/6J mice. Switching from an HF to an SC diet reduced obesity and insulin resistance, and protected against the development of NASH and liver tumourigenesis in the same mice. Moreover, *Irs1*$^{-/-}$ mice fed an HF diet were dramatically protected against NASH and liver tumourigenesis, suggesting that IRS-1 inhibition might protect against HF diet-induced NASH and liver tumourigenesis, despite the presence of insulin resistance.

Acknowledgements We thank M. Kaji and E. Sakamoto (Department of Endocrinology and Metabolism, Graduate School of Medicine, Yokohama City University, Yokohama, Japan) for their excellent technical assistance and animal care.

Funding This work was supported in part by: Grants-in-Aid for Scientific Research (B) 19390251 and (B) 21390282 from the Ministry of Education, Culture, Sports, Science and Technology (MEXT) of Japan; a Medical Award from the Japan Medical Association; a Grant-in-Aid from the Uehara Memorial Foundation; a Grant-in-Aid from the Daiichi–Sankyo Foundation of Life Science; and a Grant-in-Aid from the Naito Foundation (to Y. Terauchi).

Contribution statement All the authors conceived and designed the study, and participated in the analysis and interpretation of the data. AN drafted the manuscript, and all the other authors revised it critically for intellectual content. All the authors approved the final version of the paper.

Duality of interest The authors declare that there is no duality of interest associated with this manuscript.

References

1. Finucane MM, Stevens GA, Cowan MJ et al (2011) National, regional, and global trends in body-mass index since 1980: systematic analysis of health examination surveys and epidemiological studies with 960 country-years and 9.1 million participants. Lancet 377:557–567
2. Danaei G, Finucane MM, Lu Y et al (2011) National, regional, and global trends in fasting plasma glucose and diabetes prevalence since 1980: systematic analysis of health examination surveys and epidemiological studies with 370 country-years and 2.7 million participants. Lancet 378:31–40
3. Calle EE, Rodriguez C, Walker-Thurmond K, Thun MJ (2003) Overweight, obesity, and mortality from cancer in a prospectively studied cohort of U.S. adults. N Engl J Med 348:1625–1638
4. Inoue M, Iwasaki M, Otani T, Sasazuki S, Noda M, Tsugane S (2006) Diabetes mellitus and the risk of cancer: results from a large-scale population-based cohort study in Japan. Arch Intern Med 166:1871–1877
5. Starley BQ, Calcagno CJ, Harrison SA (2010) Nonalcoholic fatty liver disease and hepatocellular carcinoma: a weighty connection. Hepatology 51:1820–1832
6. Hill-Baskin AE, Markiewski MM, Buchner DA et al (2009) Diet-induced hepatocellular carcinoma in genetically predisposed mice. Hum Mol Genet 18:2975–2988
7. VanSaun MN, Lee IK, Washington MK, Matrisian L, Gorden DL (2009) High fat diet induced hepatic steatosis establishes a permissive microenvironment for colorectal metastases and promotes primary dysplasia in a murine model. Am J Pathol 175:355–364
8. Park EJ, Lee JH, Yu GY et al (2010) Dietary and genetic obesity promote liver inflammation and tumorigenesis by enhancing IL-6 and TNF expression. Cell 140:197–208
9. Saltiel AR, Kahn CR (2001) Insulin signalling and the regulation of glucose and lipid metabolism. Nature 414:799–806
10. Kubota N, Kubota T, Itoh S et al (2008) Dynamic functional relay between insulin receptor substrate 1 and 2 in hepatic insulin signaling during fasting and feeding. Cell Metab 8:49–64
11. Guo S, Copps KD, Dong X et al (2009) The Irs1 branch of the insulin signaling cascade plays a dominant role in hepatic nutrient homeostasis. Mol Cell Biol 29:5070–5083
12. Monetti M, Levin MC, Watt MJ et al (2007) Dissociation of hepatic steatosis and insulin resistance in mice overexpressing DGAT in the liver. Cell Metab 6:69–78
13. Chattopadhyay M, Selinger ES, Ballou LM, Lin RZ (2011) Ablation of PI3K p110-α prevents high-fat diet-induced liver steatosis. Diabetes 60:1483–1492
14. Horie Y, Suzuki A, Kataoka E et al (2004) Hepatocyte-specific Pten deficiency results in steatohepatitis and hepatocellular carcinomas. J Clin Invest 113:1774–1783
15. Kudo Y, Tanaka Y, Tateishi K et al (2011) Altered composition of fatty acids exacerbates hepatotumorigenesis during activation of the phosphatidylinositol 3-kinase pathway. J Hepatol 55:1400–1408
16. Kubota N, Tobe K, Terauchi Y et al (2000) Disruption of insulin receptor substrate-2 causes type 2 diabetes due to liver insulin resistance and lack of compensatory beta-cell hyperplasia. Diabetes 49:1880–1889
17. Terauchi Y, Matsui J, Kamon J et al (2004) Increased serum leptin protects from adiposity despite the increased glucose uptake in white adipose tissue in mice lacking p85alpha phosphoinositide 3-kinase. Diabetes 53:2261–2270

18. Kubota N, Yano W, Kubota T et al (2007) Adiponectin stimulates AMP-activated protein kinase in the hypothalamus and increases food intake. Cell Metab 6:55–68
19. Tamemoto H, Kadowaki T, Tobe K et al (1994) Insulin resistance and growth retardation in mice lacking insulin receptor substrate-1. Nature 372:182–186
20. Araki E, Lipes MA, Patti ME et al (1994) Alternative pathway of insulin signalling in mice with targeted disruption of the IRS-1 gene. Nature 372:186–190
21. Terauchi Y, Iwamoto K, Tamemoto H et al (1997) Development of non-insulin-dependent diabetes mellitus in the double knockout mice with disruption of insulin receptor substrate-1 and beta cell glucokinase genes. Genetic reconstitution of diabetes as a polygenic disease. J Clin Invest 99:861–866
22. Brown MS, Goldstein JL (2008) Selective versus total insulin resistance: a pathogenic paradox. Cell Metab 7:95–96
23. Semple RK, Sleigh A, Murgatroyd PR et al (2009) Postreceptor insulin resistance contributes to human dyslipidemia and hepatic steatosis. J Clin Invest 119:315–322
24. Biddinger SB, Hernandez-Ono A, Rask-Madsen C et al (2008) Hepatic insulin resistance is sufficient to produce dyslipidemia and susceptibility to atherosclerosis. Cell Metab 7:125–134
25. Zhang J, Ou J, Bashmakov Y, Horton JD, Brown MS, Goldstein JL (2001) Insulin inhibits transcription of IRS-2 gene in rat liver through an insulin response element (IRE) that resembles IREs of other insulin-repressed genes. Proc Natl Acad Sci USA 98:3756–3761
26. Leavens KF, Easton RM, Shulman GI, Previs SF, Birnbaum MJ (2009) Akt2 is required for hepatic lipid accumulation in models of insulin resistance. Cell Metab 10:405–418
27. Kadowaki T, Ueki K, Yamauchi T, Kubota N (2012) SnapShot: insulin signaling pathways Cell 148:624 (Abstract)
28. Rung J, Cauchi S, Albrechtsen A et al (2009) Genetic variant near IRS1 is associated with type 2 diabetes, insulin resistance and hyperinsulinemia. Nat Genet 41:1110–1115
29. Giovannucci E, Harlan DM, Archer MC et al (2010) Diabetes and cancer: a consensus report. Diabetes Care 33:1674–1685
30. Vigneri P, Frasca F, Sciacca L, Pandini G, Vigneri R (2009) Diabetes and cancer. Endocr Relat Cancer 16:1103–1123
31. Johnson JA, Pollak M (2010) Insulin, glucose and the increased risk of cancer in patients with type 2 diabetes. Diabetologia 53:2086–2088
32. Kleiner DE, Brunt EM, Van Natta M et al (2005) Design and validation of a histological scoring system for nonalcoholic fatty liver disease. Hepatology 41:1313–1321

Diabetologia (2012) 55:3318–3330
DOI 10.1007/s00125-012-2711-1

ARTICLE

Depletion of homeodomain-interacting protein kinase 3 impairs insulin secretion and glucose tolerance in mice

N. Shojima · K. Hara · H. Fujita · M. Horikoshi · N. Takahashi · I. Takamoto · M. Ohsugi · H. Aburatani · M. Noda · N. Kubota · T. Yamauchi · K. Ueki · T. Kadowaki

Received: 5 June 2012 / Accepted: 7 August 2012 / Published online: 16 September 2012

Abstract
Aims/hypothesis Insufficient insulin secretion and reduced pancreatic beta cell mass are hallmarks of type 2 diabetes. Here, we focused on a family of serine-threonine kinases known as homeodomain-interacting protein kinases (HIPKs). HIPKs are implicated in the modulation of Wnt signalling, which plays a crucial role in transcriptional activity, and in pancreas development and maintenance. The aim of the present study was to characterise the role of HIPKs in glucose metabolism.
Methods We used RNA interference to characterise the role of HIPKs in regulating insulin secretion and transcription activity. We conducted RT-PCR and western blot analyses to analyse the expression and abundance of HIPK genes and proteins in the islets of high-fat diet-fed mice. Glucose-induced insulin secretion and beta cell proliferation were measured in islets from *Hipk3*$^{-/-}$ mice, which have impaired glucose tolerance owing to an insulin secretion deficiency. The abundance of pancreatic duodenal homeobox (PDX)-1 and glycogen synthase kinase (GSK)-3β phosphorylation in *Hipk3*$^{-/-}$ islets was determined by immunohistology and western blot analyses.
Results We found that HIPKs regulate insulin secretion and transcription activity. *Hipk3* expression was most significantly increased in the islets of high-fat diet-fed mice. Furthermore, glucose-induced insulin secretion and beta cell proliferation were decreased in the islets of *Hipk3*$^{-/-}$ mice. Levels of PDX1 and GSK-3β phosphorylation were significantly decreased in *Hipk3*$^{-/-}$ islets.
Conclusions/interpretation Depletion of HIPK3 impairs insulin secretion and glucose tolerance. Decreased levels of HIPK3 may play a substantial role in the pathogenesis of type 2 diabetes.

Keywords Glucose homeostasis · Homeodomain-interacting protein kinase · Insulin secretion

Abbreviations

ChIP	Chromatin immunoprecipitation
GSK	Glycogen synthase kinase
HIPK	Homeodomain-interacting protein kinase
NK	Neurokinin
PCNA	Proliferating cell nuclear antigen
PDX	Pancreatic duodenal homeobox
SF-1	Splicing factor 1
siRNA	Small interfering RNA

Introduction

Type 2 diabetes is a complex disease characterised by chronic hyperglycaemia resulting from insulin resistance

Electronic supplementary material The online version of this article (doi:10.1007/s00125-012-2711-1) contains peer-reviewed but unedited supplementary material, which is available to authorised users.

N. Shojima · K. Hara (✉) · H. Fujita · M. Horikoshi · N. Takahashi · I. Takamoto · M. Ohsugi · N. Kubota · T. Yamauchi · K. Ueki · T. Kadowaki (✉)
Department of Diabetes and Metabolic Disease, Graduate School of Medicine, University of Tokyo, 113-8655 Hongo 7-3-1, Bunkyo-ku, Tokyo, Japan
e-mail: thara-tky@umin.ac.jp
e-mail: kadowaki-3im@h.u-tokyo.ac.jp

N. Takahashi
Center for Disease Biology and Integrative Medicine, Faculty of Medicine, University of Tokyo, Tokyo, Japan

H. Aburatani
Research Center for Advanced Science and Technology, University of Tokyo, Tokyo, Japan

M. Noda
National Center for Global Health and Medicine, Tokyo, Japan

and impaired beta cell function [1–3]. Accumulating evidence shows that Wnt signalling modulates beta cell function [4–9]. The Wnts are a family of secreted glycoproteins that influence cell development via autocrine and paracrine mechanisms [10, 11]. Activation of the canonical pathway occurs by binding of Wnt ligands to the frizzled receptor. This binding triggers an intracellular signalling cascade, which leads to serine/threonine phosphorylation, inactivation of glycogen synthase kinase (GSK)-3β and destabilisation of the destruction complex, preventing GSK3β phosphorylation of β-catenin. This mechanism enables the accumulation and nuclear translocation of β-catenin. Once inside the nucleus, β-catenin acts in combination with the T cell factor to stimulate transcription of Wnt-responsive genes.

GSK-3 was originally identified as a serine/threonine kinase that inactivates glycogen synthase. GSK3 affects many cellular processes, including transcription, cell cycle regulation and apoptosis. GSK3β has been shown to affect beta cell mass, proliferation and apoptosis [12–14].

Homeodomain-interacting protein kinases (HIPKs) are implicated in the modulation of Wnt signalling in cultured cells [15], and in mouse [16, 17], *Drosophila* [18, 19] and *Xenopus* embryos [20, 21]. Members of the HIPK family (HIPK1, HIPK2, HIPK3, HIPK4) were originally identified as binding partners of the neurokinin (NK) homeodomain protein [22]. HIPKs have been reported to be essential for coordinated death in early developmental stages and for the regulation of proper cell number in diverse tissue types. Studies have shown that the HIPK family, and in particular its most studied member, HIPK2, interact with, phosphorylate and modulate the function of other homeodomain proteins, as well as other transcription factors, including p53 [23–25] and carboxy-terminal binding protein (CtBP)-1 [26, 27]. HIPK2 has been reported to modulate the transcriptional activity of pancreatic duodenal homeobox (PDX)-1 [28], which plays a crucial role in pancreas development [29–31].

Several studies have revealed important roles of HIPK3 in the regulation of transcription and phosphorylation in cultured cells [32–36]. HIPK3 overproduction has been reported to enhance androgen receptor-dependent transcription in various cell lines [32]. HIPK3 induced Fas-associated death domain (FADD) phosphorylation and inhibited Fas-mediated Jun NH2-terminal kinase activation [33]. HIPK3 also increased splicing factor 1 (SF-1) activity for steroidogenic gene transcription in response to cAMP through phosphorylation of death-associated protein 6 [35]. Interestingly, *HIPK1*, *HIPK2* and *HIPK3* expression in islets from patients with type 2 diabetes is decreased by 32% (p=0.326), 30% (p=0.082) and 46% (p=0.064), respectively, according to data from the Diabetes Genomic Anatomic Project [3], suggesting that HIPK genes play a role in the control of beta cell function. However, the question of whether HIPKs might be involved in the effects of glucose metabolism has not been addressed.

The current study was undertaken to define the mechanisms by which HIPKs regulate glucose metabolism. Here we show that *Hipk* transcripts are expressed in pancreatic beta cells, and modulate insulin secretion and insulin promoter activity. We found that a high-fat diet enhanced *Hipk3* expression. Moreover, our analysis of *Hipk3*$^{-/-}$ mice revealed that they had impaired glucose tolerance due to a deficiency of insulin secretion. We also demonstrated that levels of PDX1 and phosphorylation of GSK3β were significantly decreased in *Hipk3*$^{-/-}$ islets. Hence, our data provide evidence of a new mechanism by which insulin secretion is regulated.

Methods

RT-PCR Total RNA was isolated from mouse islets and mouse pancreas using TRIzol reagent (Invitrogen, Carlsbad, CA, USA). RT-PCR was performed using reverse transcriptase (RevTraAce; Toyobo, Osaka, Japan). The RT-PCR products were amplified using ExTaq polymerase (Takara, Kyoto, Japan). The gene-specific primer pairs were used, as previously described [37].

Quantitative RT-PCR Quantification of the selected genes was performed using TaqMan gene expression assays with a commercially available system (7900HT; Applied Biosystems, Foster City, CA, USA). For each gene, an assay was selected to amplify the region corresponding to the location of the relevant probe. Gene expression analysis was performed using commercially available mouse assays as follows: *Hipk1*: Mm00501689_m1; *Hipk2*: Mm00439329_m1; *Hipk3*: Mm00468880_m1; *Pdx1*: Mm00435565_m1; *Gck*: Mm00439129_m1; *Slc2a2*: Mm00446229_m1; Cyclin D1: Mm00432359_m1; *Hnf4* (also known as *Hnf4a*): m00433964_m1; *Tcf7l2*: Mm00501505_m1; *Irs2*: Mm03038438_m1; *Ins1*: Mm01950294_s1; *Ins2*: Mm00731595_g1; *Hnf1a*: Mm00493434_m1; *Hnf1b*: Mm00447459_m1; *Irs1*: Mm01278327_m1; *Ucp2*: Mm00627599_m1; and *Gapdh*: Mm99999915_g1 (Applied Biosystems). The assays for *Gapdh* and *Pdx1* were performed in parallel as controls. Standard TaqMan cycling conditions were used and all reactions were performed in triplicate. Changes in expression levels in quantitative PCR were calculated as $2^{-\Delta\Delta C_t}$ (cycle threshold) values and presented relative to average changes.

Immunoprecipitation and immunoblotting analysis of mouse islets Polyclonal anti-PDX1, anti-hepatocyte nuclear factor 4 alpha, anti-GSK3β, anti-phospho-GSK3β(Ser9), anti-β-catenin and anti-α-tubulin antibodies were purchased from Santa Cruz Biotechnology (Santa Cruz, CA, USA). Polyclonal anti-IRS2 antibodies were purchased from Cell Signaling Technology (Beverly, MA, USA). Islets were sonicated, using

an ultrasound sonicator, in 300 to 500 μl ice-cold buffer containing: 0.5% (vol./vol.) Triton X-100, 50 mmol/l TRIS-HCl (pH 8.0), 100 mmol/l NaCl, 1 mmol/l EDTA, 1 mmol/l Na_3VO_4, 10 mmol/l NaF and 1 mmol/l phenylmethylsulfonyl fluoride. Supernatant fractions were cleared at 12,000*g* for 5 min, and incubated with protein A-Sepharose and each specific antibody. Samples were separated by SDS-polyacrylamide gel electrophoresis and immunodetection performed with a kit (ECL; Amersham Bioscience, Arlington Heights, IL, USA). Protein was prepared from more than 100 islets pooled from several mice of identical genotype.

RNA interference and transient transfection Small interfering RNA (siRNA)-Lipofectamine 2000 complexes were prepared using 50 nmol/l siRNA for Hipk genes (Stealth Select RNAi; Invitrogen) and control siRNA (Invitrogen). Islets were precultured for 24 h, medium was changed to OptiMEM (Invitrogen) and siRNA-Lipofectamine 2000 complexes with or without DNA-Lipofectamine 2000 complexes were added. After 8 h incubation, the transfection medium was aspirated and replaced, for an additional 48 h, with fresh culture medium containing 2.8 mmol/l glucose.

Luciferase assays Insulin reporter constructs were constructed from rat pancreas cDNA and genomic DNA using Advantage2 Taq (Invitrogen). The luciferase reporter plasmid harbouring the 5′-flanking region of rat *Ins1* exon 1 (−450 to 51) was subcloned into the pGL4 vector (Promega Biosciences, Madison, WI, USA). Islets plated on to a 24 well plate were transfected with 0.5 μg of each luciferase reporter plasmid and 0.02 μg Renilla luciferase plasmid with the herpes simplex virus thymidine kinase promoter (phRL-TK) using Lipofectamine 2000. Cells were collected 48 h after transfection and luciferase assays were carried out (Promega).

Chromatin immunoprecipitation assay Assays were performed in mouse islets. A chromatin immunoprecipitation (ChIP) assay kit (Upstate, Lake Placid, NY, USA) was used according to procedures suggested by the manufacturer. After crossing and sonication, cell lysates were immunoprecipitated with the indicated antibodies. The eluted genomic DNA from immunoprecipitates was subjected to PCR amplification. Anti-HIPK1, anti-HIPK2, anti-HIPK3 and anti-PDX1 antibodies, as well as control rabbit IgG (Santa Cruz Biotechnology) were used in ChIP assays. For PCR primer sequences, see electronic supplementary material (ESM) Table 1.

Analysis of Hipk3$^{-/-}$ *mice* Mice deficient for *Hipk3* were generated using the gene trapping method developed by Lexicon Genetics (Woodlands, TX, USA) and supplied by CLEA (Tokyo, Japan). The artificial DNA was designed such that it could be inserted randomly into any gene, preventing the RNA splicing mechanism from working properly and thereby knocking out the gene's function. The inserted DNA was specifically engineered to disrupt the function of the trapped gene, activate a selectable marker, enable the generation of knockout mice and allow precise identification of the chromosomal insertion site (www.lexpharma.com/research/drug-discovery/gene-knockouts.html, last accessed 8 August 2012). Mice were 8 to 20 weeks of age at the time of the experiment. Male 8-week-old BKS. Cg-+*Lepr*^{db}/+*Lepr*^{db}/Jcl (*db/db*) mice and BKS. Cg-*m*+/*m*+/Jcl mice (control) were purchased (CLEA). We used a high-fat diet consisting of 32% fat, 25.5% (wt/wt) protein, 2.9% fibre, 4.0% ash, 29.4% carbohydrates and 6.2% water (CLEA). For all other experiments, the diet consisted of standard chow (CLEA) with the following composition: 25.6% (wt/wt) protein, 3.8% fibre, 6.9% ash, 50.5% carbohydrates, 4% fat and 9.2% water.

Mice were fasted for >16 h before the glucose tolerance test, then loaded with 1.5 mg/g body weight glucose by oral or intraperitoneal administration. Blood samples were collected from the orbital sinus at various time points and glucose measured using an automatic blood glucose meter (Glutest Ace; Sanwa Kagaku, Nagoya, Japan). Insulin and GLP-1 levels were determined using a mouse insulin ELISA kit (Shibayagi, Shibukawa, Japan) and GLP-1 ELISA kit (Wako, Osaka, Japan), respectively. Mice were intraperitoneally challenged with 0.75 mU/g body weight human insulin (Novolin R; Novo Nordisk, Bagsvaerd, Denmark) in an insulin tolerance test. Animal care and the procedures of the experiments were approved by the Animal Care Committee of the University of Tokyo.

Histological and immunohistochemical analysis of mouse islets Female mice (n=4) aged 8 to 20 weeks were used for each genotype and 20 sections of islets were evaluated for morphometry. We studied four animals each per genotype and diet. Analysis was based on cell counts ranging from 1,500 to 2,000 per control and transgenic mouse islet samples. Tissues were routinely processed for paraffin embedding, and 4 μm sections were cut and mounted on silanised slides. Pancreatic sections were stained with anti-insulin, anti-HIPK3 anti-proliferating cell nuclear antigen (PCNA), anti-PDX1 and anti-phspho-GSK3β antibodies. Non-specific staining was blocked by 2 mg/ml poly-L-lysine pre-absorption [38]. Images of pancreatic tissue and islet beta cells were viewed on the monitor of a computer through a microscope connected to a charge-coupled device camera (Olympus, Tokyo, Japan). The areas of the pancreas, beta cells and non-beta cells were traced manually and analysed with Win ROOF software (Mitani, Fukui, Japan).

Islet isolation and culture Mouse pancreas was incubated for 30 min at 37°C in 2.5 ml KRB buffer containing collagenase

(Sigma-Aldrich, St Louis, MO, USA). The pancreas was dispersed by pipetting and washed twice with KRB buffer. Mouse recombinant Wnt3a was purchased from Wako. Glibenclamide, LiCl and 1-azakenpaullone were purchased form Sigma-Aldrich. Static incubation was performed for 1 h at 37°C with ten islets per tube after 20 min of preincubation. Insulin levels were determined with a mouse insulin ELISA kit (Shibayagi). For the perifusion experiment, ten islets of similar size were maintained in KRB buffer delivered using a peristaltic pump. Perifusion was as follows: 30 min with KRB buffer containing 2.8 mmol/l glucose; 20 min with KRB buffer containing 20 mmol/l glucose; 40 min with KRB buffer containing 2.8 mmol/l glucose; 10 min with KRB buffer containing 2.8 mmol/l KCl; and 30 min with KRB buffer containing 2.8 mmol/l glucose. Perifusate was collected every 5 min. At the end of the perifusion, islets were collected by handpicking and extracted with 0.18 mol/l HCl in 70% ethanol for determination of insulin content.

ATP measurement ATP measurement of islets was performed as previously described with some modifications [39]. After preincubation, 1 ml fresh KRB buffer containing 2.8, 10 or 22 mmol/l glucose was introduced. Incubation was carried out for 1 h at 37°C and stopped by adding trichloroacetic acid. ATP content of the cells was assayed in duplicate by the luminometric method using an ATP bioluminescent assay kit (Sigma).

Two-photon excitation imaging Two-photon excitation imaging of islets was performed as previously described [40]. Ca^{2+} measurements were performed using fura-2 as the Ca^{2+} indicator. Fura-2 post-stimulation fluorescence (F) was normalised to the resting fluorescence ($F0$). The increase of Ca^{2+} concentration was calculated as $(F0-F)/F0$.

Statistical analysis All data are presented as the mean± SEM of independent replicates. All statistical analyses were performed by one-way ANOVA or χ^2 analysis as indicated.

Results

The reduction of Hipk1, Hipk2 and Hipk3 expression by RNA interference attenuates insulin secretion We assessed the expression of Hipk family genes by RT-PCR using cDNA prepared from isolated mouse islets. Hipk family expression was detected in islets (Fig. 1a). Quantitative RT-PCR using TaqMan gene expression assays revealed that the expression of *Hipk2* and *Hipk3* was two- and 2.5-fold higher, respectively, than that of *Hipk1* (Fig. 1b,c). We estimated whether Hipk genes can also decrease insulin secretion from isolated islets. siRNA to *Hipk1*, *Hipk2* and *Hipk3* suppressed endogenous expression by 45%, 44% and 46%, respectively (Fig. 1d), leading upon stimulation with 20 mmol/l glucose to decreases in insulin secretion by 42%, 44% and 46%, respectively (Fig. 1d). We also found that simultaneous inhibition of *Hipk1* and *Hipk2*, *Hipk2* and *Hipk3*, and *Hipk1* and *Hipk3* inhibited insulin secretion by 52%, 54% and 56%, respectively (Fig. 1e). Simultaneous inhibition of *Hipk1*, *Hipk2* and *Hipk3* inhibited insulin secretion by 78% (Fig. 1e). These observations suggest that the additive inhibition of Hipk genes leads to impaired beta cell function. To evaluate whether Hipk genes also affect insulin promoter transcriptional activity, we conducted luciferase assays using RNA interference approaches. siRNA to *Hipk1*, *Hipk2* and *Hipk3* decreased insulin promoter transcriptional activity in isolated mouse islets by 38%, 44% and 52%, respectively (Fig. 1f). Endogenous insulin transcript levels were assessed by quantitative RT-PCR and correlated with the results obtained in luciferase reporter assays (Fig. 1g). ChIP assay revealed that HIPKs interacted with the insulin promoter (Fig. 1h).

Hipk family expression in the islets of mice fed a high-fat diet mRNA expression of *Hipk1*, *Hipk2*, and *Hipk3* was increased in the extracts of islets isolated from B6 mice fed a high-fat diet for 12 weeks, compared with islets from control chow-fed B6 mice. Increases were by 44%, 78% and 109%, respectively (Fig. 2a). HIPK1, HIPK2 and HIPK3 levels were increased by 41%, 98% and 112%, respectively, in the extracts of islets isolated from B6 mice fed a high-fat diet (Fig. 2b), indicating that HIPK3 accumulation may correlate with glucose tolerance in this environmental model of type 2 diabetes.

Hipk3 expression is enhanced in the islets of db/db mice We examined *Hipk3* expression in *db/db* mice. *Hipk3* mRNA was increased by 96% and 54%, respectively, in the extracts of islets isolated from 8- and 20-week-old *db/db* mice compared with 8-week-old control mouse islets (Fig. 2c). HIPK3 protein was increased by 94% and 51%, respectively, in the extracts of islets isolated from 8- and 20-week-old *db/db* mice compared with 8-week-old control mouse islets (Fig. 2d). We also performed immunohistochemical analysis, finding that HIPK3 levels were increased in islets from *db/db* mice (Fig. 2e). This indicates that HIPK3 accumulation correlates with glucose tolerance in this genetic model of type 2 diabetes.

$Hipk3^{-/-}$ mice had impaired insulin secretion To elucidate the physiological role of HIPK3 in glucose metabolism, we examined the phenotypes of *$Hipk3^{-/-}$* mice. *$Hipk3^{-/-}$* mice showed normal weight gain on a standard and a high-fat diet (Fig. 3a). Their overall appearance at death after 12 weeks on a high-fat diet revealed no difference between *$Hipk3^{-/-}$* and wild-type mice on either a standard or a high-fat diet. We performed the OGTT on mice fed a standard diet. *$Hipk3^{-/-}$* mice fed a standard diet had significantly impaired

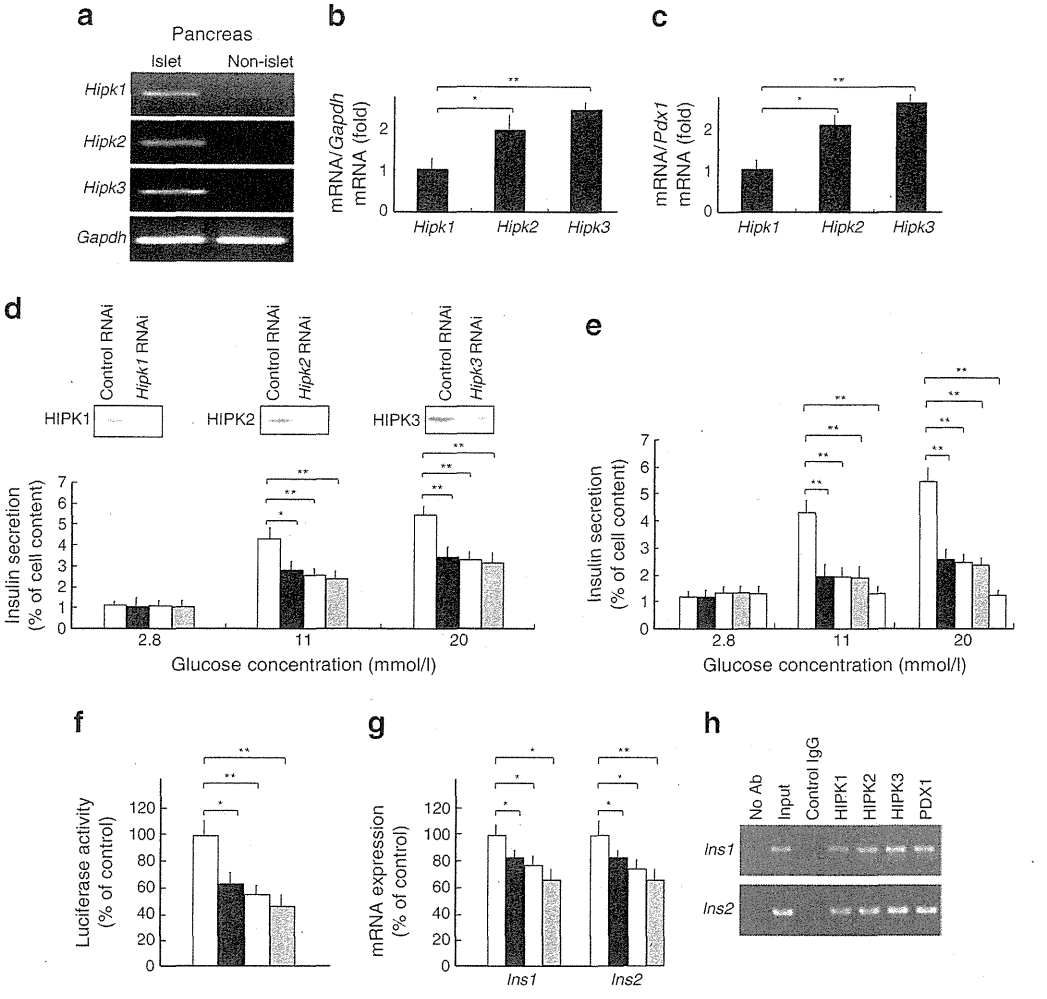

Fig. 1 (**a**) RT-PCR analysis of Hipk genes in islets isolated from a wild-type mouse. Quantitative RT-PCR using TaqMan gene expression assays was performed to validate the relative expression of Hipk genes. (**b**) Assays for *Gapdh* and (**c**) *Pdx1* were performed in parallel as control. (**d**) Blots showing *Hipk1*, *Hipk2* and *Hipk3* inactivation by RNA interference (RNAi). siRNA-Lipofectamine 2000 complexes were prepared (n=4), and suppression of glucose-stimulated insulin secretion by gene inactivation was quantified. White bars, control; black bars, *Hipk1*; light grey bars, *Hipk2*; dark grey bars, *Hipk3*. (**e**) Glucose-stimulated insulin secretion was decreased by a combination of *Hipk1*, *Hipk2* and *Hipk3* RNA interference treatment (n=4). White bars, control; black bars, *Hipk1*+*Hipk2*; mid-grey bars, *Hipk2*+*Hipk3*; dark grey bars, *Hipk1*+*Hipk3*; light grey bars, *Hipk1*+*Hipk2*+*Hipk3*. (**f**) Insulin promoter transcriptional activity was suppressed by *Hipk1*, *Hipk2* and *Hipk3* inactivation by RNA interference in mouse isolated islets. Islets were precultured for 24 h, and DNA-Lipofectamine 2000 complexes along with siRNA-Lipofectamine 2000 complexes were added (n=4). Isolated islets were transfected with 0.1 μg of the rat insulin I promoter luciferase reporter plasmid pINS (−450 to 51)-pGL4 and by siRNA to *Hipk1*, *Hipk2* and *Hipk3*, and control siRNA. Luciferase activity was measured 48 h after transfection. Key as above (**d**). (**g**) Endogenous insulin transcript levels were assessed by quantitative RT-PCR. Key as in (**d**). (**h**) The recruitment of HIPKs on the *Ins1* and *Ins2* promoter in mouse islets. ChIP assays were performed in islets using the indicated antibodies (Ab) and primer pairs. As controls, PCR reactions were performed with input DNA (lane 2), DNA immunoprecipitated by rabbit IgG (lane 3) and DNA that was immunoprecipitated in the absence of antibody (lane 1). Data represent the average results from three independent ChIP experiments. Data (**a**–**g**) are from three independent islet preparations and experiments, with measurements in duplicate, and are presented as mean±SEM: *p<0.05 and **p<0.01 compared with control siRNA

glucose tolerance (Fig. 3b) and decreased insulin response to glucose (Fig. 3c) compared with wild-type mice. Under standard diet conditions, intraperitoneal glucose tolerance and glucose-dependent insulin secretion of *Hipk3*$^{-/-}$ mice were similar to those of wild-type mice (Fig. 3b). *Hipk3*$^{-/-}$ mice had significantly impaired GLP-1 secretion during an OGTT compared with that of wild-type mice (Fig. 3d). *Hipk3*$^{-/-}$ mice fed a high-fat diet for 4 and 12 weeks had significantly impaired glucose tolerance (Fig. 3e, f) and decreased insulin response to glucose (Fig. 3g, h, k) compared with wild-type mice. The glucose-lowering effect of insulin did not differ between *Hipk3*$^{-/-}$ and wild-type mice on a standard or a high-fat diet (Fig. 3i, j, l), supporting the hypothesis that glucose intolerance in *Hipk3*$^{-/-}$ mice was

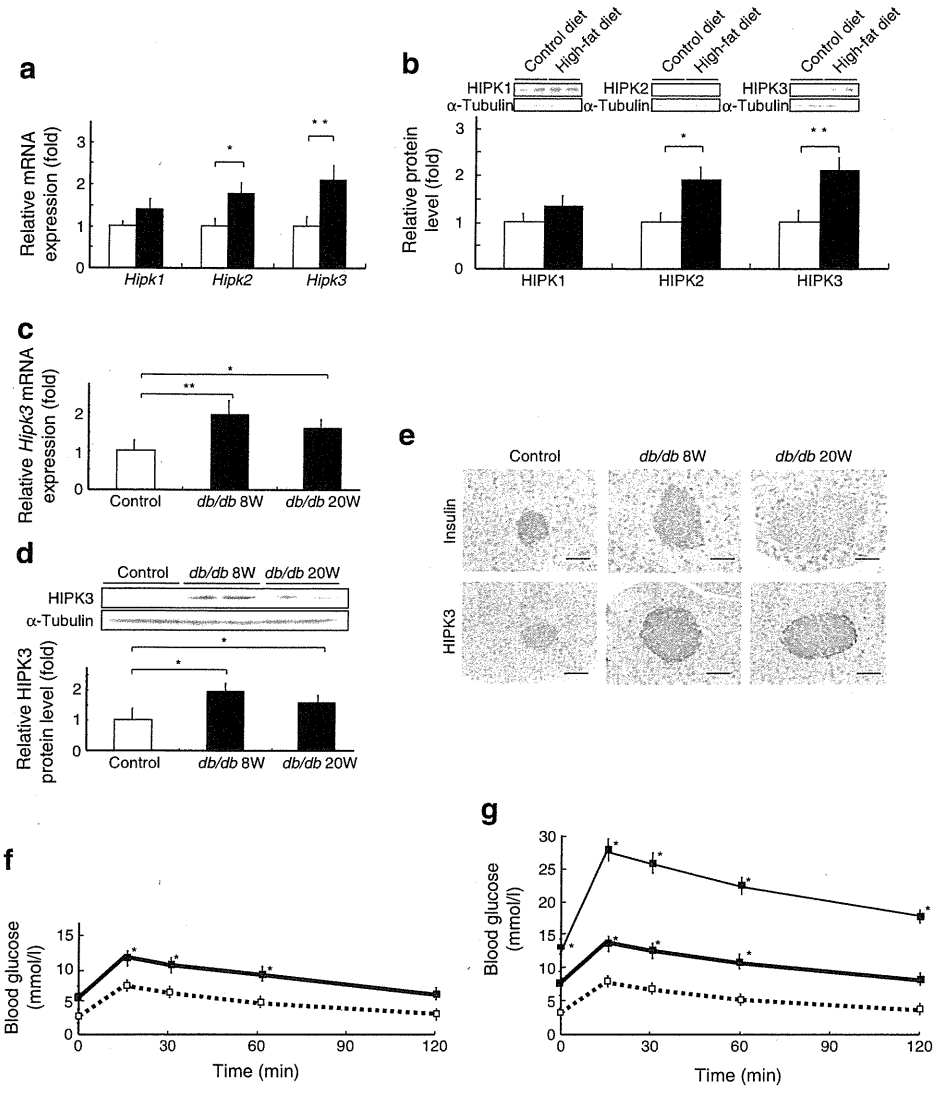

Fig. 2 Changes in Hipk genes mRNA expression (**a**) and protein (**b**) abundance in islets from mice fed a high-fat (black bars; white bars, control) diet (n=4). Quantitative RT-PCR analysis of *Hipk3* was done in islets isolated from wild-type mice. Protein was prepared from more than 100 islets pooled from several mice. Protein samples from lysates of isolated islets were immunoprecipitated using anti-HIPK1, -HIPK2 and -HIPK3 antibodies, and separated by SDS-PAGE. Western blot analyses were performed with the same antibodies. (**c**) Changes to *Hipk3* mRNA expression and (**d**) protein levels in islets from 8-week-old (8W) and 20-week-old (20W) *db/db* mice (n=4). RT-PCR analysis of *Hipk3* was done in islets isolated from wild-type mice. Samples were normalised using α-tubulin. Protein samples from lysates of isolated islets were separated by SDS-PAGE and western blot analyses performed using anti-HIPK3 antibody. (**e**) Immunohistochemical analysis of paraffin-embedded sections from 8- and 20-week-old *db/db* mice using anti-insulin and anti-HIPK3 antibodies. Scale bars, 100 μm. (**f**) OGTT results for mice fed a high-fat diet (continuous black line; dotted line, control diet) and (**g**) for *db/db* mice (dotted line, control; thick black line, *db/db* 8 weeks old; thin black line, *db/db* 20 weeks old). Data represent means±SEM; *p<0.05 and **p<0.01 compared with control

not the result of major differences in insulin responsiveness to glucose.

Loss of Hipk3 decreases glucose-induced insulin secretion We next determined glucose-induced insulin secretion in *Hipk3*$^{-/-}$ mice by static incubation of the same numbers of islets. Whereas insulin secretion into the medium by islets from *Hipk3*$^{-/-}$ and wild-type mice was similar at 2.8 mmol/l glucose, insulin secretion by islets from *Hipk3*$^{-/-}$ mice was significantly decreased at 11 and 20 mmol/l glucose compared with islets from wild-type mice (Fig. 4a). However, the secretory response in *Hipk3*$^{-/-}$ mouse islets was restored by treatment with KCl or glibenclamide (Fig. 4b). To characterise the molecular defect in insulin secretion, we performed pancreas perifusion experiments. In *Hipk3*$^{-/-}$ mice, the insulin secretory response to 20 mmol/l glucose was delayed and decreased